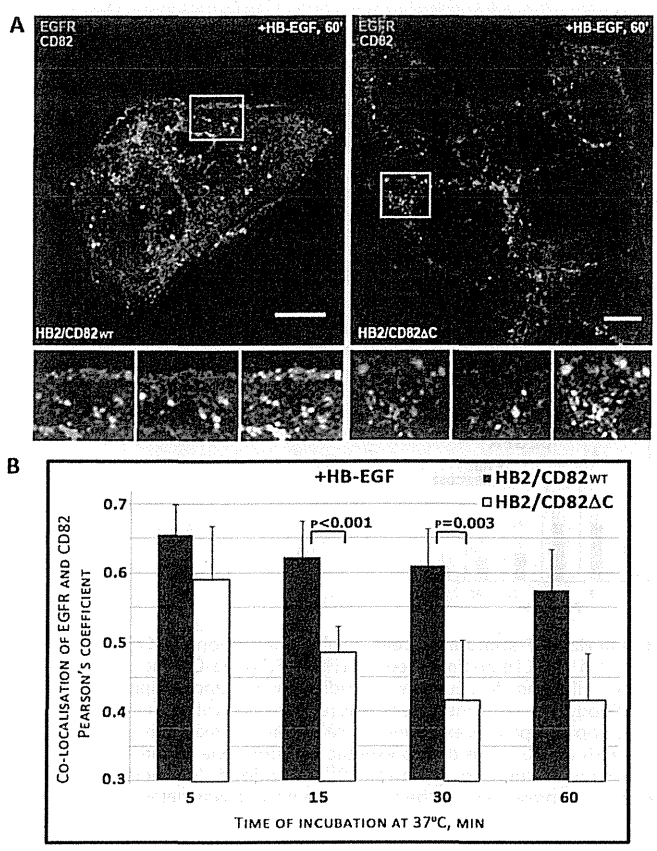

FIGURE 6. **Co-localization of internalized CD82 and EGFR after HB-EGF stimulation.** HB2/CD82 and HB2/CD82ΔC cells were incubated with HB-EGF (25 ηg/ml) and anti-CD82 mAb (TS82b) at 4 °C for 1 h. After three washes, the cells were chased at 37 °C for the indicated time intervals. The cells were fixed, permeabilized, and co-stained with anti-EGFR mAb. Co-localization of CD82 and EGFR was assessed using isotype specific Alexa Fluor-conjugated goat anti-mouse antibodies. *A*, representative confocal images of cells following 60 min of chase are presented. *Scale bar*, 10 μm. *B*, quantification of co-localized EGFR and CD82 after internalization was calculated in an average 40–50 cells at each time point in each cell line after collection of z-sections. The data are presented as Pearson's coefficient. The values are means from three independent experiments. The *p* values were determined by paired two-tailed *t* test.

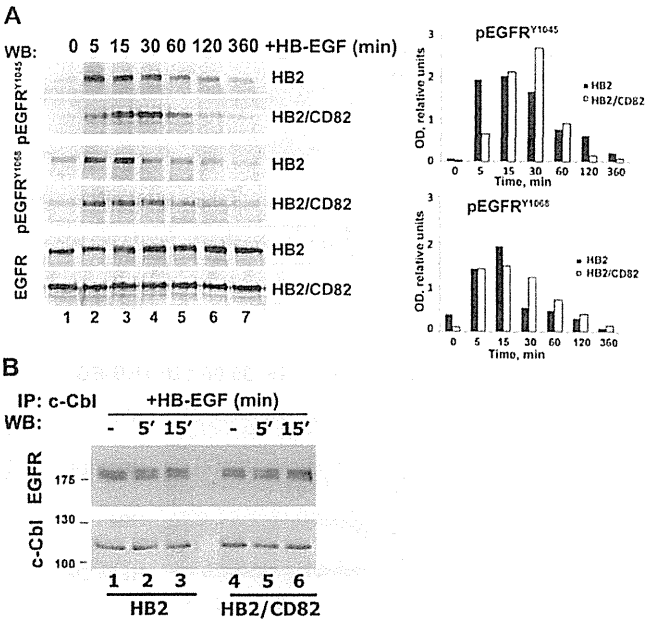

FIGURE 7. **CD82 and recruitment of c-Cbl to HB-EGF-stimulated EGFR.** *A*, serum-starved HB2 and HB2/CD82 cells were incubated with HB-EGF (15 ηg/ml) at 37 °C for indicated time intervals. Equal amounts of protein (~10 μg) were loaded onto polyacrylamide gels, and kinetics of phosphorylation was determined by Western blotting (*WB*) with the appropriate antibodies. Blots were developed using HRPO-conjugated secondary antibody from Dako. The levels of total EGFR were also tested. The data presented are from one of three independent experiments. Quantification of this experiment is shown in a graph. Densitometry was carried out using ImageJ. *B*, interaction of c-Cbl with EGFR in HB-EGF-stimulated cells was studied by immunoprecipitation (*IP*) with anti-c-Cbl antibody. EGFR was detected by Western blotting with anti-EGFR polyclonal antibody as described under "Experimental Procedures." The same membrane was redeveloped with anti-c-Cbl goat antibody. The results of a representative experiment are shown (three in total).

was considerably decreased with the corresponding difference being more than 33%. These data indicate that the C-terminal region is important for a prolonged association of CD82 with EGFR in endocytic compartments, and the divergence in trafficking routes between the wild type protein and the mutant may, indeed, underlie the functional deficiency of the CD82ΔC toward EGFR after HB-EGF stimulation.

CD82 Regulates Serine Phosphorylation of c-Cbl in HB-EGF-stimulated Cells: the Role of PKC—Ligand-induced ubiquitylation of EGFR is dependent on the interaction of Cbl E3 ubiquitin ligases with the activated receptor (17). Phosphorylation of the receptor on Tyr^{1045} and Tyr^{1068} leads to the direct or indirect (via Grb2) recruitment of c-Cbl (28). First, we studied HB-EGF induced phosphorylation of EGFR on Tyr^{1045} and Tyr^{1068} in both HB2/CD82 and control cells (Fig. 7*A*). Although there were minor variations in phosphorylation at individual time points, we observed no consistent differences in kinetics of Tyr^{1068} phosphorylation between the cell lines. On the other hand, presence of CD82 affected the kinetics of Tyr^{1045} phosphorylation. In the control cells, phosphorylation of Tyr^{1045} peaked at 5–15 min (Fig. 7*A*, *top panel*). This correlated with the kinetics of ubiquitylation of HB-EGF-activated receptor in HB2 cells (see above). In contrast, phosphorylation of the receptor on this residue in HB2/CD82 cells was minimal at the 5-min time point and then steadily increased up to 30 min (Fig. 7*A*). Notably, phosphorylation of Tyr^{1045} at the 5-min time point in HB2/CD82 cells was ~2.5 times lower when compared with control cells (Fig. 7*A*, compare *lane 2, two top panels*). We also observed that decay of Tyr^{1045} phosphorylation was faster in CD82-expressing cells over extended time course (Fig. 7*A*, *lanes 6* and *7, two top panels*). Notably, despite these differences, the interaction between EGFR and c-Cbl was not affected by either the presence of CD82 or the treatment of cells with HB-EGF (Fig. 7*B*). Therefore, we concluded that CD82 dependent differences in ubiquitylation are not due to differential assembly of the EGFR-Cbl complex in the control and HB2/CD82 cells.

The activity of c-Cbl is regulated by tyrosine and serine phosphorylation of the protein (29, 30). Thus, we investigated whether phosphorylation of c-Cbl upon HB-EGF stimulation is affected in the presence of CD82. Although we observed no qualitative or quantitative differences in phosphorylation of c-Cbl on tyrosines 774 and 731 in HB2 and HB2/CD82 cells

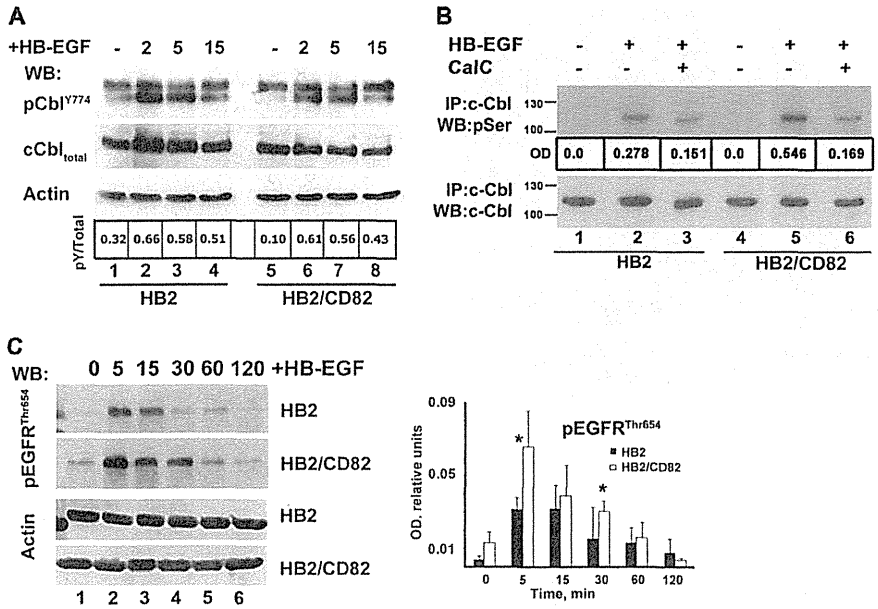

FIGURE 8. **CD82 modulates PKC-dependent phosphorylation of EGFR and c-Cbl in HB-EGF-stimulated cells.** *A*, phosphorylation of c-Cbl on Tyr^{774} was studied by Western blotting (*WB*) with phosphospecific anti-Cbl antibody in cells (HB2 and HB2/CD82) stimulated with HB-EGF. Total c-Cbl and actin were used as control for loading. *B*, serine phosphorylation of c-Cbl in HB-EGF-stimulated cells (HB2 and HB2/CD82) was studied by immunoprecipitation (*IP*) with anti-c-Cbl mAb followed by Western blotting with anti-phosphoserine polyclonal antibody. The same membrane was redeveloped with anti-c-Cbl polyclonal antibody to confirm that equal amount of protein was immunoprecipitated in each sample. In parallel experiments, cells were pretreated for 1.5 h with 5 μM (final concentration) of anti-PKC inhibitor Calphostin C (*CalC*) before stimulation with HB-EGF. The data presented are from one of three independent experiments. *C*, phosphorylation of EGFR on Thr^{654} was studied by Western blotting with phosphospecific anti-$EGFR^{Thr654}$ antibody (Millipore). The blot is a representative of three independent experiments. Quantification of three experiments is presented on the graph. The *p* value was determined in paired two-tailed *t* test.

(Fig. 8*A*, and data not shown), HB-EGF-induced serine phosphorylation of c-Cbl was more pronounced (by ~2-fold) in CD82-expressing cells (Fig. 8*B*, *lanes 2* and *5*). PKCα has been reported to phosphorylate c-Cbl on serine residues (30, 31). Given that CD82 is known to recruit PKC to plasma membrane (32), we investigated to what degree PKC is responsible for serine phosphorylation of c-Cbl in HB-EGF-stimulated cells. We used the specific inhibitor of PKC Calphostin C for treating control and CD82-expressing cells before and during stimulation with HB-EGF. Serine phosphorylation of c-Cbl was decreased by almost 3-fold in HB2/CD82 cells compared with 1.5-fold in control cells (Fig. 8*B*, *lanes 3* and *6*). We concluded that PKC contributes to serine phosphorylation of c-Cbl following HB-EGF phosphorylation, and this is more pronounced in the presence of CD82.

To explore the connection between CD82, PKC and ubiquitylation of EGFR further, we analyzed phosphorylation of the receptor on Thr^{654}. PKC-dependent phosphorylation of this residue in the juxtamembrane domain of EGFR has been previously linked with suppression of EGFR ubiquitylation and diversion of receptor trafficking toward recycling (33, 34). We found that phosphorylation of EGFR on Thr^{654} was significantly increased in CD82-expressing cells after stimulation with HB-EGF (more than 2-fold at the 5-min time point) (Fig. 8*C*, *lane 2*, *top two panels*). Furthermore, Thr^{654} phosphorylation lasted longer in HB2/CD82 cells when compared with the control cells (Fig. 8*C*, *lanes 4–6*). Taken together, these data indicate that CD82 can regulate HB-EGF-induced ubiquitylation of EGFR at multiple levels through mechanisms involving PKC.

DISCUSSION

The role of tetraspanin proteins in regulation of various signal transduction pathways has been well documented (3). It has been proposed that tetraspanins function via specialized membrane microdomains by modulating activities of the associated signaling receptors (*e.g.*, integrins, ErbB proteins). Here we describe a novel pathway that implicates tetraspanins in regulation of ubiquitylation of their molecular partners. Specifically, we demonstrate that the metastasis suppressor tetraspanin KAI-1/CD82 controls ligand-induced ubiquitylation of EGFR.

Perhaps one of our most intriguing discoveries is a specific effect of CD82 on ubiquitylation and trafficking of EGFR activated by growth factors with heparin-binding domains (HB-EGF and AR). Variations in ubiquitylation of EGFR were attributed to differences in affinities of specific ligand-receptor pairs (26, 27). Our results show for the first time that ligand-dependent differential ubiquitylation of EGFR is also controlled by CD82, a tetraspanin protein, which we previously described as a molecular partner for the receptor (5). Furthermore, CD82-dependent molecular mechanisms (discussed below) are unlikely to rely on either differential ligand affinities or pH sensitivities of HB-EGF/AR-EGFR complexes. Indeed, we found that HB-EGF-induced phosphorylation of the receptor's autophosphorylation site Tyr^{1068} at the early time points was comparable in both cell lines, thereby excluding the differences in ligand binding.

It has been previously reported that different ligands dictate the postendocytic itinerary of activated EGF receptor (26), and this correlates with the extent of EGFR ubiquitylation upon

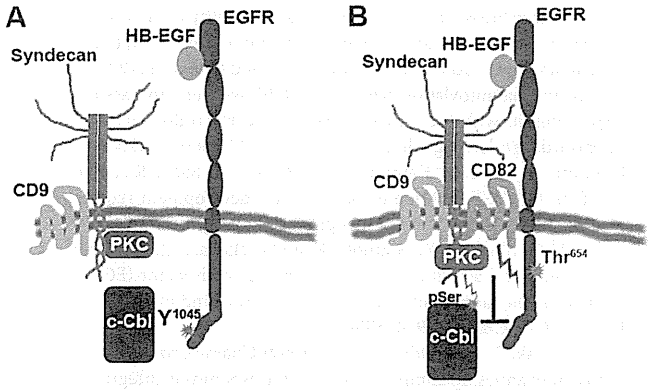

FIGURE 9. **CD82 links HSPG-activated PKC, ligand-bound EGFR and c-Cbl.** The model depicts the role of CD82 in early events of EGFR activation by heparin-binding domain containing ligand (*e.g.*, HB-EGF). *A*, in absence of CD82 EGFR is not recruited to the tetraspanin-enriched microdomains. HB-EGF binding leads to robust phosphorylation of the receptor, recruitment of c-Cbl, and further ubiquitylation. *B*, when CD82 is expressed, a subset of EGFR associated with the tetraspanin is recruited to TERM where it is placed in close proximity to syndecans. Stimulation with HB-EGF leads to activation of PKC recruited to TERM by syndecans and CD82. PKC attenuates EGFR signaling by affecting c-Cbl recruitment to this subset of receptors. Additionally, active PKC negatively regulates activity of E3 ligase by serine/threonine phosphorylation.

ligand binding. Although more pronounced ubiquitylation is typically linked to increased targeting of the receptor to lysosomes (26), it has been also reported that the level of ubiquitylation does not always correlate with degradation of EGFR (35). Indeed, our results show that despite differences in EGFR ubiquitylation, total levels of the receptor in HB2 and HB2/CD82 cells remain similar and unchanged over the extended period of exposure to HB-EGF (Fig. 7*A*). Thus, our data indicate that CD82-dependent differences in HB-EGF-induced ubiquitylation most likely affect trafficking pathways preceding lysosomal targeting of EGFR.

What could be the mechanisms underlying the regulatory specificity of CD82 toward ligand-induced ubiquitylation of EGFR? Our data with sΔHB variant of HB-EGF strongly suggest that CD82 acts via HSPG. Binding of many heparin-binding growth factors including HB-EGF and AR to their receptors is influenced by HSPG (21, 36, 37). These ligand-HSPG interactions may either enhance or attenuate the activity of the receptors (20, 21). Importantly, it has previously been reported that the activity of HB-EGF (but not EGF) is dependent on syndecans, the most prominent family of cell-associated proteoglycans (38, 39). Therefore, one can envisage a scenario whereby CD82 and its tetraspanin partners (*e.g.*, CD9, which is known to associate with syndecans (3, 5)) facilitate formation of the tripartite EGFR-growth factor-HSPG complex, which activates not only receptor but also HSPG. CD82 and activated HSPG (*e.g.*, syndecans) could, in turn, recruit PKCα (40, 41), thereby increasing effective concentration of the enzyme in proximity to its targets (*i.e.*, EGFR, c-Cbl). Consequently, increased phosphorylation of threonine 654 in EGFR on one hand and serine phosphorylation of c-Cbl on the other would lead to changes in both ligand-induced ubiquitylation of the receptor and alteration of its postendocytic trafficking route (33) (Fig. 9). Although the proposed model explains the regulatory specificity of CD82 toward various EGFR ligands (indeed, the activity of CD82 can be observed only when growth factors engage HSPG), future work will be required to establish molecular mechanisms underlying the CD82-dependent functional dynamics between the complexes of HSPG-PKC on one side and EGFR-c-Cbl on the other.

We found that reduction of HB-EGF-induced ubiquitylation of EGFR also influenced its intracellular trafficking: dynamics of receptors' recruitment to the early/sorting endosomes and their egress from these compartments were changed in CD82-expressing cells. The timing of EGFR co-localization with EEA1-containing endosomes was delayed, which could be due to the altered ubiquitylation and subsequent endocytosis of the receptors associated with HSPG in TERM. Syndecans are known to mediate endocytosis of heparin-binding ligands and proteins (*e.g.*, FGF2 or eosinophil cationic protein) by macropinocytosis (42, 43). This pathway is slow and involves formation of uncoated vesicles that eventually fuse with sorting endosomes. The fate of the cargo-HSPG complex is decided according to the ubiquitylation status of cargo or HSPG (*e.g.*, syndecans) interactions (44, 45) and may progress either to the lysosomal degradation or to the recycling route (44). The role of CD82 in this diversion could be in bringing EGFR in proximity to HSPG and regulating ubiquitylation on one side (discussed above) and in providing suitable lipid surroundings (*e.g.*, gangliosides and/or cholesterol content) on the other (6).

Our report demonstrates for the first time the functional importance of the C-terminal cytoplasmic part of CD82: deletion of this region compromises the activity of this tetraspanin toward EGFR upon stimulation with HB-EGF. Importantly, functional deficiency of CD82ΔC correlates with changes in the endocytic trafficking of this mutant. First, we found that the C-terminal cytoplasmic region regulates internalization of CD82. Given that this part of the protein carries a "classical" tyrosine-based motif (YSKV), the involvement of AP-2 and, consequently, clathrin would be anticipated. However, our electron microscopy data clearly demonstrate that CD82 is excluded from the clathrin-coated pits and coated vesicles. These results further strengthen a recent observation by Xu *et al.* (15), who showed that CD82 is internalized via clathrin- and dynamin-independent pathway(s). Second, we found that endocytosed CD82ΔC mutant (but not the wild type protein) is concentrated in the polymorphic compartment close to the plasma membrane. Although the exact identity of these structures remains unknown, these results strongly suggest that the C-terminal region of CD82 also contributes to postendocytic trafficking of the protein. How does the deficiency in trafficking affect the activity of CD82ΔC toward EGFR? We observed that the time of co-localization with the HB-EGF-activated receptor is decreased for the mutant when compared with the wild type CD82. Hence, a possible physical link between HB-EGF-bound EGFR and HSPG (see above) may also be short-lived (or destabilized) in CD82ΔC-expressing cells.

In summary, our results describe CD82 as a novel regulator of ligand-induced ubiquitylation of EGF receptor. This newly established activity of CD82 suggests a new paradigm in tetraspanin-dependent regulation of endocytic trafficking of the associated transmembrane cargos. Although HB-EGF is a potent mitogen for various cell types, its binding may also lead

to decreased proliferation in certain cellular contexts (20). Although the underlying mechanisms of the HB-EGF opposing activities are still unknown, it is not unfeasible that the differential expression of CD82 and its involvement in ligand-induced ubiquitylation of EGFR is, in fact, a critical factor that controls the alternative signaling pathways.

Acknowledgments—We are grateful to all our colleagues for providing antibodies and reagents. We thank Drs. Cindy Miranti and Eric Rubinstein for valuable discussions and advice. We thank Alexandra Berditchevskaia for editorial help.

REFERENCES

1. Berditchevski, F. (2001) Complexes of tetraspanins with integrins. More than meets the eye. *J. Cell Sci.* **114,** 4143–4151
2. Hemler, M. (2003) Tetraspanin proteins mediate cellular penetration, invasion, and fusion events and define a novel type of membrane microdomain. *Annu. Rev. Cell Dev. Biol.* **19,** 397–422
3. Charrin, S., le Naour, F., Silvie, O., Milhiet, P.-E., Boucheix, C., and Rubinstein, E. (2009) Lateral organisation of membrane proteins. tetraspanins spin their web. *Biochem. J.* **420,** 133–154
4. Berditchevski, F., and Odintsova, E. (2007) Tetraspanins as regulators of protein trafficking. *Traffic* **8,** 89–96
5. Odintsova, E., Sugiura, T., and Berditchevski, F. (2000) Attenuation of EGF receptor signaling by a metastasis suppressor, the tetraspanin CD82/KAI-1. *Curr. Biol.* **10,** 1009–1012
6. Odintsova, E., Butters, T. D., Monti, E., Sprong, H., van Meer, G., and Berditchevski, F. (2006) Gangliosides play an important role in the organization of CD82-enriched microdomains. *Biochem. J.* **400,** 315–325
7. He, B., Liu, L., Cook, G. A., Grgurevich, S., Jennings, L. K., and Zhang, X. A. (2005) Tetraspanin CD82 attenuates cellular morphogenesis through down-regulating integrin alpha6-mediated cell adhesion. *J. Biol. Chem.* **280,** 3346–3354
8. Sridhar, S. C., and Miranti, C. K. (2006) Tetraspanin KAI1/CD82 suppresses invasion by inhibiting integrin-dependent crosstalk with c-Met receptor and Src kinases. *Oncogene* **25,** 2367–2378
9. Takahashi, M., Sugiura, T., Abe, M., Ishii, K., and Shirasuna, K. (2007) Regulation of c-Met signaling by the tetraspanin KAI-1/CD82 affects cancer cell migration. *Int. J. Cancer* **121,** 1919–1929
10. Miranti, C. K. (2009) Controlling cell surface dynamics and signalling. How CD82 suppresses metastasis. *Cell. Signal.* **21,** 196–211
11. Tsai, Y. C., and Weissman, A. M. (2011) Dissecting the diverse functions of the metastasis suppressor CD82/KAI1. *FEBS Lett.* **585,** 3166–3173
12. Danglot, L., Chaineau, M., Dahan, M., Gendron, M. C., Boggetto, N., Perez, F., and Galli, T. (2010) Role of TI-VAMP and CD82 in EGFR cell-surface dynamics and signaling. *J. Cell Sci.* **123,** 723–735
13. Escola, J. M., Kleijmeer, M. J., Stoorvogel, W., Griffith, J. M., Yoshie, O., and Geuze, H. J. (1998) Selective enrichment of tetraspan proteins on the internal vesicles of multivesicular endosomes and on exosomes secreted by human B-lymphocytes. *J. Biol. Chem.* **273,** 20121–20127
14. Vyas, J. M., Kim, Y.-M., Artavanis-Tsakonas, K., Love, J. C., Van der Veen, A. G., and Ploegh, H. L. (2007) Tubulation of class II MHC compartments is microtubule dependent and involves multiple endolysosomal membrane proteins in primary dendritic cells. *J. Immunol.* **178,** 7199–7210
15. Xu, C., Zhang, Y. H., Thangavel, M., Richardson, M. M., Liu, L., Zhou, B., Zheng, Y., Ostrom, R. S., and Zhang, X. A. (2009) CD82 endocytosis and cholesterol-dependent reorganization of tetraspanin webs and lipid rafts. *FASEB J.* **23,** 3237–3288
16. Sigismund, S., Confalonieri, S., Ciliberto, A., Polo, S., Scita, G., and Di Fiore, P. P. (2012) Endocytosis and signaling. Cell logistics shape the eukaryotic cell plan. *Physiol. Rev.* **92,** 273–366
17. Sorkin, A., and Goh, L. K. (2009) Endocytosis and intracellular trafficking of ErbBs. *Exp. Cell Res.* **315,** 683–696
18. Shearer, M., Bartkova, J., Bartek, J., Berdichevsky, F., Barnes, D., Millis, R., and Taylor-Papadimitriou, J. (1992) Studies of clonal cell lines developed from primary breast cancers indicate that the ability to undergo morphogenesis in vitro is lost early in malignancy. *Int. J. Cancer* **51,** 602–612
19. Berditchevski, F., Odintsova, E., Sawada, S., and Gilbert, E. (2002) Expression of the palmitoylation-deficient CD151 weakens the association of $\alpha 3\beta 1$ integrin with the tetraspanin-enriched microdomains and affects integrin-dependent signaling. *J. Biol. Chem.* **277,** 36991–37000
20. Iwamoto, R., Mine, N., Kawaguchi, T., Minami, S., Saeki, K., and Mekada, E. (2010) HB-EGF function in cardiac valve development requires interaction with heparan sulfate proteoglycans. *Development* **137,** 2205–2214
21. Takazaki, R., Shishido, Y., Iwamoto, R., and Mekada, E. (2004) Suppression of the biological activities of the epidermal growth factor (EGF)-like domain by the heparin-binding domain of heparin-binding EGF-like growth factor. *J. Biol. Chem.* **279,** 47335–47343
22. Berditchevski, F., and Odintsova, E. (1999) Characterization of integrin-tetraspanin adhesion complexes. Role of tetraspanins in integrin signaling. *J. Cell Biol.* **146,** 477–492
23. Bolte, S., and Cordelières, F. P. (2006) A guided tour into subcellular colocalisation analysis in light microscopy. *J. Microsc.* **224,** 213–232
24. Kleijmeer, M. J., Raposo, G., and Geuze, H. J. (1996) Characterization of MHC class II compartments by immunoelectron microscopy. *Methods* **10,** 191–207
25. Liou, W., Geuze, H. J., and Slot, J. W. (1996) Improving structural integrity of cryosections for immunogold labeling. *Histochem. Cell Biol.* **106,** 41–58
26. Roepstorff, K., Grandal, M. V., Henriksen, L., Knudsen, S. L., Lerdrup, M., Grøvdal, L., Willumsen, B. M., and van Deurs, B. (2009) Differential effects of EGFR ligands on endocytic sorting of the receptor. *Traffic* **10,** 1115–1127
27. Baldys, A., Göoz, M., Morinelli, T. A., Lee, M.-H., Raymond, J. R. Jr., Luttrell, L. M., and Raymond, J. R., Sr. (2009) Essential role of c-Cbl in amphiregulin-induced recycling and signaling of the endogenous epidermal growth factor receptor. *Biochemistry* **48,** 1462–1473
28. Roepstorff, K., Grøvdal, L., Grandal, M., Lerdrup, M., and van Deurs, B. (2008) Endocytic downregulation of ErbB receptors. Mechanisms and relevance in cancer. *Histochem. Cell Biol.* **129,** 563–578
29. Swaminathan, G., and Tsygankov, A. Y. (2006) The Cbl family proteins. Ring leaders in regulation of cell signalling. *J. Cell. Physiol.* **209,** 21–43
30. Pedraza-Alva, G., Sawasdikosol, S., Liu, Y. C., Mérida, L. B., Cruz-Muñoz, M. E., Oceguera-Yañez, F., Burakoff, S. J., and Rosenstein, Y. (2001) Regulation of Cbl molecular interactions by the co-receptor molecule CD43 in human T cells. *J. Biol. Chem.* **276,** 729–737
31. Melander, F., Andersson, T., and Dib, K. (2004) Engagement of $\beta 2$ integrins recruits 14-3-3 proteins to c-Cbl in human neutrofils. *Biochem. Biophys. Res. Commun.* **317,** 1000–1005
32. Zhang, X. A., Bontrager, A. L., and Hemler, M. E. (2001) Transmembrane-4 superfamily proteins associate with activated protein kinase C (PKC) and link PKC to specific β_1 integrins. *J. Biol. Chem.* **276,** 25005–25013
33. Bao, J., Alroy, I., Waterman, H., Schejter, E. D., Brodie, C., Gruenberg, J., and Yarden, Y. (2000) Threonine phosphorylation diverts internalised epidermal growth factor receptors from a degradative pathway to the recycling endosome. *J. Biol. Chem.* **275,** 26178–26186
34. Cotton, C. U., Hobert, M. E., Ryan, S., and Carlin, C. R. (2013) Basolateral EGF receptor sorting regulated by functionally distinct mechanisms in renal epithelial cells. *Traffic* **14,** 337–354
35. Stern, K. A., Place, T. L., and Lill, N. L. (2008) EGF and amphiregulin differentially regulate Cbl recruitment to endosomes and EGF receptor fate. *Biochem. J* **410,** 585–594
36. Forsten-Williams, K., Chu, C. L., Fannon, M., Buczek-Thomas, J. A., and Nugent, M. A. (2008) Control of growth factor networks by heparan sulfate proteoglycans. *Ann. Biomed. Eng.* **36,** 2134–2148
37. Gitay-Goren, H., Soker, S., Vlodavsky, I., and Neufeld, G. (1992) The binding of vascular endothelial growth factor to its receptors is dependent on cell-surface-associated heparin-like molecules. *J. Biol. Chem.* **267,** 6093–6098
38. Higashiyama, S., Abraham, J. A., and Klagsbrun, M. (1993) Heparin-binding EGF-like growth factor stimulation of smooth muscle cell migration. Dependence on interactions with cell surface heparan sulfate. *J. Cell Biol.* **122,** 933–940

39. Mahtouk, K., Cremer, F. W., Rème, T., Jourdan, M., Baudard, M., Moreaux, J., Requirand, G.,Fiol, G., De Vos, J., Moos, M., Quittet, P., Goldschmidt, H., Rossi, J. F., Hose, D., and Klein, B. (2006) Heparan sulfate proteoglycans are essential for the myeloma cell growth activity of EGF-family ligands in multiple myeloma. *Oncogene* **25,** 7180–7191
40. Couchman, J. R. (2010) Transmembrane signalling. Proteoglycans. *Annu. Rev. Cell Dev. Biol.* **26,** 89–114
41. Keum, E., Kim, Y., Kim, J., Kwon, S., Lim, Y., Han, I., and Oh, E.-S. (2004) Syndecan-4 regulates localization, activity and stability of protein kinase C-α. *Biochem. J.* **378,** 1007–1014
42. Fan, T.-C., Chang, H.-T., Chen, I-W., Wang, H.-Y., and Chang, M. D.-T. (2007) A heparan sulfate-facilitated and raft-dependent macropinocytosis of eosinophil cationic protein. *Traffic* **8,** 1778–1795
43. Tkachenko, E., Lutgens, E., Stan, R.-V., and Simons, M. (2004) Fibroblast growth factor 2 endocytosis in endothelial cells proceed via syndecan-4-dpendent macropinocytic pathway. *J. Cell Sci.* **117,** 3189–3199
44. Lambaerts, K., Wilcox-Adelman, S. A., and Zimmermann, P. (2009) The signalling mechanisms of syndecan heparan sulfate proteoglycans. *Curr. Opin. Cell Biol.* **21,** 662–669
45. Clague, M. J., Liu, H., and Urbé, S. (2012) Governance of endocytic trafficking and signaling by reversible ubiquitylation. *Dev. Cell* **23,** 457–467

Worm 2:1, e23415; January/February/March 2013; © 2013 Landes Bioscience

Co-occurrence of tetraspanin and ROS generators

Conservation in protein cross-linking and other developmental processes

Hiroki Moribe[1,*] and Eisuke Mekada[2]

[1]Department of Biology; Kurume University School of Medicine; Fukuoka, Japan; [2]Department of Cell Biology; Research Institute for Microbial Diseases; Osaka University; Osaka, Japan

Keywords: reactive oxygen species, cuticle, cross-linking, dual oxidase, BLI-3, tetraspanin, TSP-15, convergent evolution

Abbreviations: ROS, reactive oxygen species; H_2O_2, hydrogen peroxide; DUOX, dual oxidase; DUOXA, dual oxidase activator/dual oxidase maturation factor; NOX, NADPH oxidase; TGase, transglutaminase; TEM/TERM, tetraspanin-enriched microdomain; ECM, extracellular matrix

Submitted: 12/09/12

Accepted: 12/21/12

http://dx.doi.org/10.4161/worm.23415

*Correspondence to: Hiroki Moribe; Email: himoribe@med.kurume-u.ac.jp

Commentary to: Moribe H, Konakawa R, Koga D, Ushiki T, Nakamura K, Mekada E. Tetraspanin is required for generation of reactive oxygen species by the dual oxidase system in Caenorhabditis elegans. PLoS Genet 2012; 8:e1002957; PMID:23028364; http://dx.doi.org/10.1371/journal.pgen.1002957.

The nematode exoskeleton, commonly called the cuticle, is a highly structured extracellular matrix mainly composed of collagen. Secreted collagen molecules from the underlying epidermal cells are cross-linked via their tyrosyl residues. Reactive oxygen species (ROS) are required for the cross-linking reaction to produce tyrosyl radicals. The conserved ROS generator enzyme in *C. elegans*, BLI-3/CeDUOX1, a homolog of dual oxidases (DUOXs), is responsible for production of hydrogen peroxide. The ROS generation system must be properly controlled since ROS are highly reactive molecules that irreversibly inhibit the functions of cellular components such as nucleic acids and proteins. We recently reported that the ROS generation system directed by BLI-3 requires the tetraspanin protein, TSP-15. Herein we outline the process of cuticle development with a focus on the molecular roles of TSP-15 in the BLI-3 system. We also propose the co-occurrence of tetraspanin and ROS generators by convergent evolution.

Collagen Biosynthetic Pathway in Cuticle Development

Nematode cuticle possesses both toughness and flexibility, which protects internal tissues from adverse environments, maintains body morphology and mechanically supports locomotion via attachment to body wall muscle. Cuticle is predominantly composed of collagens encoded by over 170 genes in the *C. elegans* genome. Collagens are synthesized in underlying epidermal cells, the hypodermis and seam cells, covering almost the entire body. The collagen biosynthetic pathway is a multistep processes involving modification, folding, cleavage and secretion directed by a number of enzymes and molecular chaperons.[1] The importance of the co- and post-translational processing of collagen proteins has been supported by a comprehensive study of their mutants.[2] Gain- or reduction/loss of function of the genes relevant to collagen processing are often associated with body morphological defects represented as dumpy (Dpy), roller (Rol), squat (Sqt), blister (Bli) and molting defect (Mlt). In the final events of processing, collagen triple helices are secreted from the epidermis and are extracellularly cross-linked. Each collagen helix is covalently cross-linked via tyrosine residues resulting in the formation of dityrosine and trityrosine, which are unusual non-reducible bonds in vertebrates (see below). In *C. elegans*, tyrosine cross-linking of collagens is established by ROS-mediated catalysis driven by the BLI-3/CeDUOX1 system.[3-5] BLI-3 is a homolog of vertebrate dual oxidases that are members of the NADPH oxidase (NOX) family comprising NOX1–5 and DUOX1–2. These proteins are ROS generators that deliberately produce ROS for cellular signaling and anti-microbial responses.[6-9]

Identity and Difference of the Cross-Linking Process in Mammalian and Nematode Skin

Both nematode and mammalian skin layers share common structural

characteristics, but mammalian skin is a more complex structure. It is composed of multilayered live and dead keratinocytes that constitute a cornified layer that faces the external side.[10] Cross-linking of proteins such as involucrin and loricrin in the cornified layer is also essential for the function of mammalian skin as an external barrier. Transglutaminases (TGases) play a primary role in the cross-linking process, which catalyzes the formation of non-reducible covalent bonds between lysine and glutamate.[11] Although tyrosine cross-linkages are found in other structural proteins at low frequency and are known as biomarkers of oxidative stress and aging, little is known about their physiological role in mammals.[12] Hydroxyl lysine and lysine between collagen helices are cross-linked by lysyl oxidase in vertebrates. Lysyl oxidase-mediated cross-linkages were not found in the *C. elegans* cuticle, but they do contribute to cross-linking of type IV collagen in the basement membrane.[13,14] Interestingly, both TGases- and ROS-mediated cross-linking is observed in the formation of the fertilization envelope in sea urchin egg.[15]

Tetraspanin is a New Component of the BLI-3/CeDUOX1-ROS-Generating System

Historically, ROS have been considered deleterious by-products produced by aerobic metabolism or by exogenous stresses such as UV light and radiation, which inflict oxidative damage to organisms. The physiological role of ROS was originally believed to provide an "oxidative burst" that kills invading microbes in phagocytes. H_2O_2 produced by DUOXs also has an essential role in non-phagocytic anti-microbial defense in mucosal epithelia such as the airway and gastrointestinal tract in a wide-range of animals, including mammals, fish and insects.[16,17] The critical role of H_2O_2 produced by BLI-3/CeDUOX1 in *C. elegans* innate immunity was also demonstrated.[18-21] Besides host defense, ROS act as an intracellular redox signaling molecule by modulating target proteins via modification of their free thiol groups.[22,23] In both cases, the ROS production must be strictly regulated so that it does not damage the host. The activity of the catalytic core of NOX1-3 is regulated by the recruitment of regulatory subunits to the plasma membrane.[9,24] NOX5 and DUOX1-2 contains EF-hand motifs in the cytoplasmic region and calcium (Ca^{2+}) stimulation is essential for activation. In addition, DUOXs require interaction with their maturation factor, DUOXAs, for H_2O_2 production.[25] Dual oxidase maturation factors (DUOXA1/2) dimerize with DUOXs to target DUOXs to the cell surface.[26-28]

We preciously reported that a tetraspanin protein TSP-15 is required for cuticle development for functioning as an external barrier.[29] We recently clarified that TSP-15 functions in collagen cross-linking as a component of the DUOX system.[5] Similar to mammalian DUOXs, the BLI-3 system also requires a maturation factor and cooperates with a neighboring heme peroxidase, which corresponds to DOXA-1 and MLT-7 in *C. elegans*, respectively.[4,30] *bli-3*, *doxa-1* and *mlt-7* mutants displayed the same cuticle deficiency as a *tsp-15* mutant. Cuticle disorganization in the *tsp-15* mutant is due to impaired tyrosine cross-linking during cuticle development. In addition, the *tsp-15* mutant was restored by exogenous expression of both *bli-3* and *doxa-1*, implying that these three genes are part of the same genetic pathway. We also showed requirement of TSP-15 for BLI-3 activity by heterologous reconstitution of BLI-3, TSP-15 and DOXA-1 in mammalian cells. Finally, we showed that TSP-15 forms protein complexes with BLI-3 and DOXA-1 in vitro and in vivo.

Speculation of the Molecular Role of Tetraspanin in the BLI-3 System

Despite our contributions to the field, the molecular role of TSP-15 in H_2O_2 generation by the BLI-3 system remains elusive. By immunoblot assay, TSP-15 did not alter the protein expression level of BLI-3 at the cell surface, leading us to question what molecular switch occurs within the BLI-3 system upon association with TSP-15. The tetraspanin family comprises a large group of integral membrane proteins with common secondary and tertiary structures, including four transmembrane regions, small and large extracellular loops (LEL) and conserved cysteine residues in the LEL contributing to the formation of disulfide bonds.[31,32] It is known that tetraspanins laterally associate with each other as well as numerous membrane "partner" proteins such as adhesion molecules, growth factor receptors, membrane-bound proteases, immunoglobulin superfamily proteins. Tetraspanins also interact with intracellular signaling/cytoskeletal proteins and lipids, resulting in the formation of a highly ordered lipid-protein unit referred to as a tetraspanin-enriched microdomain (TEM/TERM) or "tetraspanin web." TEM is a distinct class of membrane microdomain and a new type of signaling platform involved in cell-cell communication.[33-36] Association with tetraspanins may properly tune functions of partner proteins. However, this modulation and facilitation process is not consistent – it may differ from partner to partner. The most likely role of TEM is in spatial assembly and clustering of specific molecules that contribute to accelerating the reaction cascade and enabling additional interactions and linkage with other key molecules and substrates. If the partner proteins are relevant to cell adhesion, antigen presentation or matrix degradation, it is convincible that the compartmentalization of these responsible molecules at specialized membrane microdomains will efficiently support their function in adhesion strengthening, cell-cell communication at immune synapses or ECM degradation in tumor invasion. It may also facilitate accessibility to substrates, while segregation of partner proteins to the microdomain may prevent non-specific reactions.[37] We currently do not have enough information to provide mechanistic insights into the TSP-15 role in the BLI-3 system, however, we have several hypotheses. First, association with TSP-15 or targeting to TEM may support the subsequent recruitment of unknown factors, or it may facilitate other forms of post-translational modification on BLI-3 that is essential for BLI-3 activation. Or more directly, as reported for other NOX isozymes and their subunits, it might induce a conformational change in BLI-3 to activate it. Conversely, interaction with TSP-15 or engagement to TEM may

replace/exclude an inhibitory factor preventing non-specific activation of BLI-3. Further analysis will be required to define the molecular role of TSP-15.

Conservation of Tyrosine Cross-Linking Machinery in Other Developmental Processes in Different Species

Although it is still not known whether tetraspanin is also crucial for the mammalian DUOX pathway, conservation of involvement of tetraspanin in the ROS generation system is, at least in part, confirmed by genetic studies of pathogenic fungi. During the infection process of the rice pathogenic fungus *Magnaporthe grisea*, the attached conidium differentiates to appressorium, a specialized structure for infection. Then the appressorium develops a penetration peg and perforates the cell wall of the host tissues. It was independently demonstrated that the mutant of *M. grisea* tetraspanin (*MgPLS1*) and the ROS generator (*MgNOX2*) was non-pathogenic owing to impairment of penetration peg formation.[38,39] The pathogenicity of other parasitic fungi with an appressoria-mediated penetration strategy in different clades was also dependent on *PLS1* and *NOX2*.[40,41] Both *PLS1* and *NOX2* were identified in other types of fungi with non-pathogenic lifestyles lacking appressorium. Furthermore, the consistency of the mutant phenotype was also observed in different developmental processes in these saprophytic fungi. In *Podospora anserina* and *Neurospora crassa*, both of their corresponding mutants of *PLS1* and *NOX2* showed the same defects in the process of germination from the ascospore.[42,43] Although the molecular mechanisms of requirement of PLS1 and NOX2 in these processes are still uncertain, the recurrent involvement of tetraspanin and ROS generators in the same cellular processes in a wide range of species makes it possible that convergent evolution is responsible for the co-occurrence of this molecular machinery.[44,45]

Disclosure of Potential Conflicts of Interest

No potential conflicts of interest were disclosed.

Acknowledgments

This work was supported by a Grant-in-Aid for Young Scientists 18770171 to H.M. and by the Global COE Program (Frontier Biomedical Science Underlying Organelle Network Biology), Ministry of Education, Culture, Sports, Science and Technology (Japan).

References

1. Page AP, Johnstone IL. The cuticle. In: The C. elegans Research Community, ed. WormBook: WormBook. http://www.wormbook.org
2. Myllyharju J, Kivirikko KI. Collagens, modifying enzymes and their mutations in humans, flies and worms. Trends Genet 2004; 20:33-43; PMID:14698617; http://dx.doi.org/10.1016/j.tig.2003.11.004.
3. Edens WA, Sharling L, Cheng G, Shapira R, Kinkade JM, Lee T, et al. Tyrosine cross-linking of extracellular matrix is catalyzed by Duox, a multidomain oxidase/peroxidase with homology to the phagocyte oxidase subunit gp91*phox*. J Cell Biol 2001; 154:879-91; PMID:11514595; http://dx.doi.org/10.1083/jcb.200103132.
4. Thein MC, Winter AD, Stepek G, McCormack G, Stapleton G, Johnstone IL, et al. Combined extracellular matrix cross-linking activity of the peroxidase MLT-7 and the dual oxidase BLI-3 is critical for post-embryonic viability in *Caenorhabditis elegans*. J Biol Chem 2009; 284:17549-63; PMID:19406744; http://dx.doi.org/10.1074/jbc.M900831200.
5. Moribe H, Konakawa R, Koga D, Ushiki T, Nakamura K, Mekada E. Tetraspanin is required for generation of reactive oxygen species by the dual oxidase system in *Caenorhabditis elegans*. PLoS Genet 2012; 8:e1002957; PMID:23028364; http://dx.doi.org/10.1371/journal.pgen.1002957.
6. Bedard K, Krause KH. The NOX family of ROS-generating NADPH oxidases: physiology and pathophysiology. Physiol Rev 2007; 87:245-313; PMID:17237347; http://dx.doi.org/10.1152/physrev.00044.2005.
7. Lambeth JD. NOX enzymes and the biology of reactive oxygen. Nat Rev Immunol 2004; 4:181-9; PMID:15039755; http://dx.doi.org/10.1038/nri1312.
8. Leto TL, Morand S, Hurt D, Ueyama T. Targeting and regulation of reactive oxygen species generation by Nox family NADPH oxidases. Antioxid Redox Signal 2009; 11:2607-19; PMID:19438290; http://dx.doi.org/10.1089/ars.2009.2637.
9. Sumimoto H. Structure, regulation and evolution of Nox-family NADPH oxidases that produce reactive oxygen species. FEBS J 2008; 275:3249-77; PMID:18513324; http://dx.doi.org/10.1111/j.1742-4658.2008.06488.x.
10. Candi E, Schmidt R, Melino G. The cornified envelope: a model of cell death in the skin. Nat Rev Mol Cell Biol 2005; 6:328-40; PMID:15803139; http://dx.doi.org/10.1038/nrm1619.
11. Iismaa SE, Mearns BM, Lorand L, Graham RM. Transglutaminases and disease: lessons from genetically engineered mouse models and inherited disorders. Physiol Rev 2009; 89:991-1023; PMID:19584319; http://dx.doi.org/10.1152/physrev.00044.2008.
12. Feeney MB, Schöneich C. Tyrosine modifications in aging. Antioxid Redox Signal 2012; 17:1571-9; PMID:22424390; http://dx.doi.org/10.1089/ars.2012.4595.
13. Cox GN, Kusch M, Edgar RS. Cuticle of *Caenorhabditis elegans*: its isolation and partial characterization. J Cell Biol 1981; 90:7-17; PMID:7251677; http://dx.doi.org/10.1083/jcb.90.1.7.
14. Norman KR, Moerman DG. The *let-268* locus of *Caenorhabditis elegans* encodes a procollagen lysyl hydroxylase that is essential for type IV collagen secretion. Dev Biol 2000; 227:690-705; PMID:11071784; http://dx.doi.org/10.1006/dbio.2000.9897.
15. Wong JL, Wessel GM. Free-radical crosslinking of specific proteins alters the function of the egg extracellular matrix at fertilization. Development 2008; 135:431-40; PMID:18094022; http://dx.doi.org/10.1242/dev.015503.
16. Allaoui A, Botteaux A, Dumont JE, Hoste C, De Deken X. Dual oxidases and hydrogen peroxide in a complex dialogue between host mucosae and bacteria. Trends Mol Med 2009; 15:571-9; PMID:19913458; http://dx.doi.org/10.1016/j.molmed.2009.10.003.
17. Bae YS, Choi MK, Lee WJ. Dual oxidase in mucosal immunity and host-microbe homeostasis. Trends Immunol 2010; 31:278-87; PMID:20579935; http://dx.doi.org/10.1016/j.it.2010.05.003.
18. Chávez V, Mohri-Shiomi A, Garsin DA. Ce-Duox1/BLI-3 generates reactive oxygen species as a protective innate immune mechanism in *Caenorhabditis elegans*. Infect Immun 2009; 77:4983-9; PMID:19687201; http://dx.doi.org/10.1128/IAI.00627-09.
19. Jain C, Yun M, Politz SM, Rao RP. A pathogenesis assay using *Saccharomyces cerevisiae* and *Caenorhabditis elegans* reveals novel roles for yeast AP-1, Yap1, and host dual oxidase BLI-3 in fungal pathogenesis. Eukaryot Cell 2009; 8:1218-27; PMID:19502579; http://dx.doi.org/10.1128/EC.00367-08.
20. Hoeven Rv, McCallum KC, Cruz MR, Garsin DA. Ce-Duox1/BLI-3 generated reactive oxygen species trigger protective SKN-1 activity via p38 MAPK signaling during infection in *C. elegans*. PLoS Pathog 2011; 7:e1002453; PMID:22216003; http://dx.doi.org/10.1371/journal.ppat.1002453.
21. van der Hoeven R, McCallum KC, Garsin DA. Speculations on the activation of ROS generation in *C. elegans* innate immune signaling. Worm 2012; 1:160-3; http://dx.doi.org/10.4161/worm.19767.
22. Brown DI, Griendling KK. Nox proteins in signal transduction. Free Radic Biol Med 2009; 47:1239-53; PMID:19628035; http://dx.doi.org/10.1016/j.freeradbiomed.2009.07.023.
23. Finkel T. Signal transduction by reactive oxygen species. J Cell Biol 2011; 194:7-15; PMID:21746850; http://dx.doi.org/10.1083/jcb.201102095.
24. Lambeth JD, Kawahara T, Diebold B. Regulation of Nox and Duox enzymatic activity and expression. Free Radic Biol Med 2007; 43:319-31; PMID:17602947; http://dx.doi.org/10.1016/j.freeradbiomed.2007.03.028.
25. Grasberger H, Refetoff S. Identification of the maturation factor for dual oxidase. Evolution of an eukaryotic operon equivalent. J Biol Chem 2006; 281:18269-72; PMID:16651268; http://dx.doi.org/10.1074/jbc.C600095200.
26. Grasberger H, De Deken X, Miot F, Pohlenz J, Refetoff S. Missense mutations of dual oxidase 2 (*DUOX2*) implicated in congenital hypothyroidism have impaired trafficking in cells reconstituted with DUOX2 maturation factor. Mol Endocrinol 2007; 21:1408-21; PMID:17374849; http://dx.doi.org/10.1210/me.2007-0018.
27. Luxen S, Noack D, Frausto M, Davanture S, Torbett BE, Knaus UG. Heterodimerization controls localization of Duox-DuoxA NADPH oxidases in airway cells. J Cell Sci 2009; 122:1238-47; PMID:19339556; http://dx.doi.org/10.1242/jcs.044123.

28. Morand S, Ueyama T, Tsujibe S, Saito N, Korzeniowska A, Leto TL. Duox maturation factors form cell surface complexes with Duox affecting the specificity of reactive oxygen species generation. FASEB J 2009; 23:1205-18; PMID:19074510; http://dx.doi.org/10.1096/fj.08-120006.
29. Moribe H, Yochem J, Yamada H, Tabuse Y, Fujimoto T, Mekada E. Tetraspanin protein (TSP-15) is required for epidermal integrity in *Caenorhabditis elegans*. J Cell Sci 2004; 117:5209-20; PMID:15454573; http://dx.doi.org/10.1242/jcs.01403.
30. Donkó A, Péterfi Z, Sum A, Leto T, Geiszt M. Dual oxidases. Philos Trans R Soc Lond B Biol Sci 2005; 360:2301-8; PMID:16321800; http://dx.doi.org/10.1098/rstb.2005.1767.
31. Boucheix C, Rubinstein E. Tetraspanins. Cell Mol Life Sci 2001; 58:1189-205; PMID:11577978; http://dx.doi.org/10.1007/PL00000933.
32. Hemler ME. Tetraspanin proteins mediate cellular penetration, invasion, and fusion events and define a novel type of membrane microdomain. Annu Rev Cell Dev Biol 2003; 19:397-422; PMID:14570575; http://dx.doi.org/10.1146/annurev.cellbio.19.111301.153609.
33. Charrin S, le Naour F, Silvie O, Milhiet PE, Boucheix C, Rubinstein E. Lateral organization of membrane proteins: tetraspanins spin their web. Biochem J 2009; 420:133-54; PMID:19426143; http://dx.doi.org/10.1042/BJ20082422.
34. Hemler ME. Tetraspanin functions and associated microdomains. Nat Rev Mol Cell Biol 2005; 6:801-11; PMID:16314869; http://dx.doi.org/10.1038/nrm1736.
35. Levy S, Shoham T. The tetraspanin web modulates immune-signalling complexes. Nat Rev Immunol 2005; 5:136-48; PMID:15688041; http://dx.doi.org/10.1038/nri1548.
36. Yáñez-Mó M, Barreiro O, Gordon-Alonso M, Sala-Valdés M, Sánchez-Madrid F. Tetraspanin-enriched microdomains: a functional unit in cell plasma membranes. Trends Cell Biol 2009; 19:434-46; PMID:19709882; http://dx.doi.org/10.1016/j.tcb.2009.06.004.
37. Yáñez-Mó M, Gutiérrez-López MD, Cabañas C. Functional interplay between tetraspanins and proteases. Cell Mol Life Sci 2011; 68:3323-35; PMID:21687991; http://dx.doi.org/10.1007/s00018-011-0746-y.
38. Clergeot PH, Gourgues M, Cots J, Laurans F, Latorse MP, Pepin R, et al. *PLS1*, a gene encoding a tetraspanin-like protein, is required for penetration of rice leaf by the fungal pathogen *Magnaporthe grisea*. Proc Natl Acad Sci U S A 2001; 98:6963-8; PMID:11391010; http://dx.doi.org/10.1073/pnas.111132998.
39. Egan MJ, Wang ZY, Jones MA, Smirnoff N, Talbot NJ. Generation of reactive oxygen species by fungal NADPH oxidases is required for rice blast disease. Proc Natl Acad Sci U S A 2007; 104:11772-7; PMID:17600089; http://dx.doi.org/10.1073/pnas.0700574104.
40. Segmüller N, Kokkelink L, Giesbert S, Odinius D, van Kan J, Tudzynski P. NADPH oxidases are involved in differentiation and pathogenicity in *Botrytis cinerea*. Mol Plant Microbe Interact 2008; 21:808-19; PMID:18624644; http://dx.doi.org/10.1094/MPMI-21-6-0808.
41. Veneault-Fourrey C, Lambou K, Lebrun MH. Fungal Pls1 tetraspanins as key factors of penetration into host plants: a role in re-establishing polarized growth in the appressorium? FEMS Microbiol Lett 2006; 256:179-84; PMID:16499604; http://dx.doi.org/10.1111/j.1574-6968.2006.00128.x.
42. Lambou K, Malagnac F, Barbisan C, Tharreau D, Lebrun MH, Silar P. The crucial role of the Pls1 tetraspanin during ascospore germination in *Podospora anserina* provides an example of the convergent evolution of morphogenetic processes in fungal plant pathogens and saprobes. Eukaryot Cell 2008; 7:1809-18; PMID:18757568; http://dx.doi.org/10.1128/EC.00149-08.
43. Malagnac F, Lalucque H, Lepère G, Silar P. Two NADPH oxidase isoforms are required for sexual reproduction and ascospore germination in the filamentous fungus *Podospora anserina*. Fungal Genet Biol 2004; 41:982-97; PMID:15465387; http://dx.doi.org/10.1016/j.fgb.2004.07.008.
44. Malagnac F, Bidard F, Lalucque H, Brun S, Lambou K, Lebrun MH, et al. Convergent evolution of morphogenetic processes in fungi: Role of tetraspanins and NADPH oxidases 2 in plant pathogens and saprobes. Commun Integr Biol 2008; 1:180-1; · PMID:19704887; http://dx.doi.org/10.4161/cib.1.2.7198.
45. Moribe H, Mekada E. Tetraspanins in lower eukaryotes. In: Berditchevski F, Rubinstein E, eds. Tetraspanins: Springer, 2013; In press.

Published OnlineFirst February 26, 2013; DOI: 10.1158/1541-7786.MCR-12-0428

Molecular Cancer Research

Molecular Hierarchy of Heparin-Binding EGF-like Growth Factor–Regulated Angiogenesis in Triple-Negative Breast Cancer

Fusanori Yotsumoto, Eriko Tokunaga, Eiji Oki, et al.

Mol Cancer Res 2013;11:506-517. Published OnlineFirst February 26, 2013.

Published OnlineFirst February 26, 2013; DOI: 10.1158/1541-7786.MCR-12-0428

Molecular Cancer Research

Genomics

Molecular Hierarchy of Heparin-Binding EGF-like Growth Factor–Regulated Angiogenesis in Triple-Negative Breast Cancer

Fusanori Yotsumoto[1,5], Eriko Tokunaga[6], Eiji Oki[6], Yoshihiko Maehara[6], Hiromi Yamada[1,5], Kyoko Nakajima[4], Sung Ouk Nam[2,5], Kohei Miyata[2,5], Midori Koyanagi[3,5], Keiko Doi[3,5], Senji Shirasawa[3,5], Masahide Kuroki[1,5], and Shingo Miyamoto[2,5]

Abstract

Heparin-binding EGF-like growth factor (HB-EGF) is one of several proangiogenic factors and represents a possible therapeutic target for patients with triple-negative breast cancer (TNBC). However, the role of HB-EGF in promoting tumor aggressiveness in TNBC remains unclear. To investigate specific genes and pathways involved in TNBC tumorigenesis, we profiled gene expression changes in two TNBC cell lines under two-dimensional culture (2DC) and three-dimensional culture (3DC) and in a tumor xenograft model. We identified simultaneous upregulation of HB-EGF, VEGFA, and angiopoietin-like 4 (ANGPTL4) in 3DC and tumor xenografts, compared with 2DC. We show that HB-EGF regulates the expression of VEGFA or ANGPTL4 via transcriptional regulation of hypoxia-inducible factor-1α and NF-κB. Furthermore, suppression of VEGFA or ANGPTL4 expression enhanced HB-EGF expression, highlighting a unique regulatory loop underlying this angiogenesis network. Targeted knockdown of HB-EGF significantly suppressed tumor formation in a TNBC xenograft model, compared with individual knockdown of either VEGFA or ANGPTL4, by reducing the expression of both VEGFA and ANGPTL4. In patients with TNBC, VEGFA or ANGPTL4 expression was also significantly correlated with HB-EGF expression. Low concentrations of exogenously added HB-EGF strongly activated the proliferation of endothelial cells, tube formation, and vascular permeability in blood vessels, in a similar fashion to high doses of VEGFA and ANGPTL4. Taken together, these results suggest that HB-EGF plays a pivotal role in the acquisition of tumor aggressiveness in TNBC by orchestrating a molecular hierarchy regulating tumor angiogenesis. *Mol Cancer Res; 11(5); 506–17.* ©*2013 AACR.*

Introduction

Angiogenesis is an essential step during the initial stages of tumor development (1–3). Cancer cells acquire anchorage-independent growth and proliferate at accelerated rates by forming 3-dimensional (3D) structures. Simultaneously, cancer cells are capable of inducing neovascularization to improve the inadequate vascular supply. In normal tissue, angiogenesis is strictly regulated by the equilibrium between proangiogenic and antiangiogenic factors. Enhanced expression of proangiogenic genes can activate quiescent microvascular endothelial cells, causing them to dissociate from the cell–cell junction, migrate into the perivascular space, proliferate extensively, and form tube structures (1, 3). Antiangiogenic factors inhibit angiogenesis by modulating endothelial cell proliferation and motility (4, 5). On the other hand, hypoxia predominantly induces the aberrant expression of proangiogenic factors, such as VEGFA in cancer cells. This occurs via an increase in nonhydroxy-hypoxia-inducible factor-1α (HIF-1α) from hydroxy-HIF-1α (6). Consequently, neovascularization is triggered, leading to the formation of tumor blood vessels that are irregularly shaped, sinuous and dilated, compared with normal peripheral vessels. Thus, disruption of the balance between proangiogenic and antiangiogenic molecules is associated with tumor angiogenesis and cancer progression (1, 7).

Triple-negative breast cancer (TNBC) is defined by the absence of estrogen and progesterone receptors and HER2 and is the most lethal and aggressive subtype of breast cancer.

Authors' Affiliations: Departments of [1]Biochemistry, [2]Obstetrics and Gynecology, and [3]Cell Biology; [4]Joint Laboratory for Frontier Medical Science, Faculty of Medicine; [5]Central Research Institute for Advanced Molecular Medicine, Fukuoka University; and [6]Department of Surgery and Sciences, Graduate School of Medical Sciences, Kyushu University, Fukuoka, Japan

Note: Supplementary data for this article are available at Molecular Cancer Research Online (http://mcr.aacrjournals.org/).

F. Yotsumoto and E. Tokunaga contributed equally to this work.

Corresponding Author: Shingo Miyamoto, Department of Obstetrics and Gynecology, Faculty of Medicine, Fukuoka University, 7-45-1 Nanakuma, Jonan-ku, Fukuoka 814-0180, Japan. Phone: 81-92-801-1011; Fax: 81-92-865-4114; E-mail: smiya@cis.fukuoka-u.ac.jp

doi: 10.1158/1541-7786.MCR-12-0428

Published OnlineFirst February 26, 2013; DOI: 10.1158/1541-7786.MCR-12-0428

Treatment of patients with TNBC still poses a major challenge, owing to a persisting lack of specific targets. Recently, numerous studies have indicated that angiogenesis plays an important role in the pathogenesis of TNBC (8–10), leading to the development of a number of novel, targeted therapies. In 2008, the U.S. Food and Drug Administration approved the use of bevacizumab (Avastin; Genentech), a humanized monoclonal antibody, plus paclitaxel, as first-line therapy in patients with metastatic breast cancer. In a recent clinical trial, bevacizumab prolonged progression-free survival but not overall survival in patients with TNBC (11, 12). Sunitinib (Sutent; Pfizer), an oral multitargeted tyrosine kinase inhibitor that inhibits the VEGF and platelet-derived growth factor (PDGF) receptors, and sorafenib (Nexavar; Onyx Pharmaceuticals), a small-molecular inhibitor of the VEGF and PDGF receptors and Raf, are effective as monotherapies in certain cancers but cause severe adverse events when combined with chemotherapy (13). In TNBC, the effects of sunitinib and sorafenib on patient survival are still under evaluation in several clinical trials. Therefore, the identification of novel target molecules involved in angiogenesis and tumorigenesis in TNBC, is essential for the development of therapeutic agents targeting this aggressive breast cancer subtype.

Heparin-binding EGF-like growth factor (HB-EGF), a ligand of EGF family (14), is initially synthesized as a transmembrane protein, similar to other ligands of the EGF family (15). The membrane-bound form of HB-EGF (pro-HB-EGF) is proteolytically cleaved from the cell surface to yield the soluble form of HB-EGF (sHB-EGF). This processing step is conducted by proteases via a mechanism known as ectodomain shedding. HB-EGF has been focused on as a promising target for many types of cancers, including TNBC (16–18). NF-κB, a member of the Rel-related proteins that includes p50, p52, v-Rel, c-Rel, RelA (p65), and RelB, is a transcription factor involved in a diversity of cellular processes, including the induction of hypoxia mediated by HB-EGF (19, 20). Previous studies have shown that HB-EGF is required for anchorage-independent cell growth and subsequent angiogenesis, thus contributing to cubic structure of tumors (21, 22). In addition, HB-EGF mediates reciprocal interactions between cancer cells and neighboring fibroblasts, which in association with the proangiogenic factor, PDGF, supports cancer progression (23). HB-EGF also induces the production of VEGFA and the activation of endothelial nitric oxide synthase (eNOS) in hypoxia (24). Taken together, these data suggest that HB-EGF modulates proangiogenic factors involved in cancer progression.

In this study, we identified 3 proangiogenic factors, HB-EGF, VEGFA, and angiopoietin-like 4 (ANGPTL4), as key molecules involved in the cubic formation of TNBC cells, using gene expression profiling. In addition, we show that these 3 proangiogenic factors cooperate to promote tumorigenesis and angiogenesis of TNBC. Importantly, however, only inhibition of HB-EGF, but not VEGFA or ANGPTL4, led to the complete suppression of tumor formation in TNBC.

Materials and Methods

Reagents and antibodies

Antibodies used in this study included goat polyclonal anti-HB-EGF (sc-1413) and rabbit polyclonal anti-ANGPTL4 (sc-66806; Santa Cruz Biotechnology); rabbit polyclonal anti-VEGFA (ab46154; Abcam); rat anti-mouse CD31 (BD Pharmingen); Alexa Fluor 555–conjugated goat anti-rat immunoglobulin G (IgG; Invitrogen Corp.); fluorescein isothiocyanate (FITC)–conjugated goat anti-rabbit IgG and FITC-conjugated rabbit anti-goat IgG (Vector Laboratories); rabbit polyclonal anti-HIF-1α and rabbit monoclonal antihydroxy-HIF-1α (Pro564; Cell Signaling Technology Inc.); mouse monoclonal anti-β-actin (Sigma-Aldrich); and peroxidase-conjugated anti-mouse IgG and peroxidase-conjugated anti-rabbit IgG (Amersham Corp.). Recombinant human proteins included: HB-EGF (259-HE; R&D Systems Inc.); VEGFA (H00007422-P01), and ANGPTL4 (H00051129-P01; Abnova Corp.). Other reagents included: 4′,6-diamidino-2-phenylindole (DAPI; Sigma-Aldrich); N-[(phenylmethoxy)carbonyl]-L-leucyl-N-[(1R)-1-formyl-3-methylbutyl]-L-leucinamide (MG132), proteasome inhibitor, and dimethyloxalyl glycine (DMOG), hydroxylase inhibitor (Cayman Chemicals).

Cell lines and cell culture

The TNBC cell lines, MDA-MB-231 and Hs578T, were purchased from the American Type Culture Collection (ATCC). MDA-MB-231 cells were grown in Leibovitz's L-15 medium (ATCC) supplemented with 10% (v/v) FBS (ICN Biomedical), 100 U/mL penicillin, and 100 μg/mL streptomycin (Invitrogen) in a humidified atmosphere at 37°C. Hs578T cells were grown in Dulbecco's modified Eagle's medium (DMEM; Nacalai Tesque, Inc.) supplemented with 10% (v/v) FBS, 10 μg/mL insulin (Sigma-Aldrich), 100 U/mL penicillin, and 100 μg/mL streptomycin in a humidified atmosphere of 5% CO_2 at 37°C. Human umbilical vein endothelial cells (HUVEC) were obtained from Clonetics Cambrex and grown in endothelial growth media (EGM) supplemented with 2% (v/v) FBS, bovine brain extract, recombinant human EGF, hydrocortisone, gentamicin, and amphotericin B according to the manufacturer's instructions in a humidified atmosphere of 5% CO_2 at 37°C. For all experiments, HUVECs were used at passage 4 or less. For the 2-dimensional culture (2DC) experiments, 1×10^5 cells were seeded in 6-well plates. For the 3D culture (3DC), cells were cultured in 10-cm dishes (50%–60% confluence) and incubated for 24 hours. Cells were then detached with trypsin–EDTA, washed 3 times with medium containing 10% (v/v) FBS, and suspended to a final concentration of 1×10^5 cells/1.5 mL. Aliquots (1.5 mL) were plated in 6-well plates precoated with 1.5 mL Matrigel (Biocoat Cellware; Becton Dickinson). Cells were incubated overnight and medium was removed and replaced with fresh medium. Cells from 3DC were retrieved from colonies using BD Cell Recovery Solution (Biocoat Cellware). Cells were

Published OnlineFirst February 26, 2013; DOI: 10.1158/1541-7786.MCR-12-0428

counted and RNA and protein extracts were prepared for downstream quantitative real-time PCR (qRT-PCR), expression array, and immunoblot analysis.

Xenograft model

Cells (5×10^6) were subcutaneously inoculated into 4-week-old nonobese diabetic/severe combined immunodeficient (NOD/SCID) mice (Charles River Laboratories Japan Inc.). To obtain total RNA for qRT-PCR and expression array analysis, tumors were resected when individual tumor volumes reached approximately 100 mm^3 and were frozen and fractured with liquid nitrogen. To assess the effects of short hairpin RNA (shRNA)–mediated knockdown of HB-EGF, VEGFA, or ANGPTL4 on tumorigenesis, tumor volume was measured once a week. Measurement of tumor size commenced after the tumor volume exceeded 100 mm^3. Each tumor volume was estimated from 2D tumor measurements as follows: tumor volume (mm^3) = length $\times$ width^2/2.

Quantitative real-time PCR

RNA extraction, cDNA synthesis, and RT-PCR were conducted as previously described (17). Expression of glyceraldehyde-3-phosphate dehydrogenase (*GAPDH*), EGF receptor (*EGFR*), *VEGFA*, *ANGPTL4*, *PDGFB*, *HIF-1α*, and *NF-κB* were detected with Assays-on-Demand primer and probe sets Hs99999905_m1, Hs00193306_m1, Hs00900054_m1, Hs01101127_m1, Hs00966522_m1, Hs00936371_m1, and Hs00765730_m1, respectively (Applied Biosystems). The procedures used for TaqMan qRT-PCR analyses and the sequences of the oligonucleotide primer pairs, TaqMan probes for HB-EGF and amphiregulin (AREG; ref. 17). mRNA expression levels for individual genes are represented as relative expression units (REU). The mRNA expression index (E.I.) was calculated as follows: E.I. = (copy number of each gene mRNA/copy number of *GAPDH* mRNA) $\times$ 10,000. The REU was determined using the E.I. of 2DC cells as a baseline (1.0).

Expression array analysis

Gene expression arrays were conducted using Human Genome U133 Plus 2.0 Array 6800 GeneChips (Affymetrix) and were analyzed by GeneSpring v7.3 software (Agilent Technologies) as previously described (25).

Measurement of soluble HB-EGF, VEGFA, ANGPTL4, PDGFAB, and PDGFBB in cell culture

The levels of HB-EGF, VEGFA, ANGPTL4, PDGFAB, and PDGFBB in the culture medium of cells were determined using a commercially available sandwich ELISA (DuoSet Kit; R&D Systems Inc.) according to the manufacturer's instructions.

Immunoblot analysis

To detect hydroxy- or nonhydroxy-HIF-1α proteins, cells were treated with 10 μmol/L MG132 or both 10 μmol/L MG132 and 1 mmol/L DMOG, respectively, for 4 hours. Cells were then rinsed with PBS containing 1 mmol/L sodium orthovanadate and lysed with 500 μL of radioimmunoprecipitation assay (RIPA) buffer to obtain total cellular protein. Cell lysates were centrifuged at 15,000 $\times$ *g* for 15 minutes at 4°C. The supernatant was boiled for 5 minutes at 95°C with 250 μL of 3$\times$ Laemmli sample buffer. All samples were subjected to SDS-PAGE and immunoblotting analyses as described previously (16).

siRNA transfection

Control siRNA (Stealth RNAi Negative Control) and siRNAs for HB-EGF, VEGFA, ANGPTL4, HIF-1α, and NF-κB p65 were purchased from Invitrogen Corp. The sequences of siRNAs used in this study are shown in Supplementary Tables S1 and S2. Cells were seeded in 10-cm dishes (50%–60% confluence) and transfected with individual siRNAs (50 nmol/L) using Lipofectamine RNAiMAX Transfection Reagent (Invitrogen Corp.) according to the manufacturer's instructions. After 24-hour incubation, the cells were subjected to 3DC.

NF-κB phosphorylation

The 3DC cells were cultured with control vehicle 0.1% (v/v) dimethyl sulfoxide (DMSO) or NF-κB p65 (Ser529/536) inhibitor peptide (Imgenex) at a final concentration of 1 μmol/L. After 48-hour incubation, cells were washed with cold PBS and lysed in 200 μL lysis buffer (Cell Signaling Technology) containing phenylmethylsulfonylfluoride (PMSF; 1 mmol/L) and protease inhibitors (1 tab/10 mL lysis buffer). Cell lysates were centrifuged at 4°C and supernatants stored at −80°C until analysis using PathScan Inflammation MultiTarget Sandwich ELISA Kit or PathScan phospho-NF-κB p65 (Ser536) Sandwich ELISA Kit according to the manufacturer's protocol (Cell Signaling Technology).

shRNA transduction using lentiviral particles

Mission Lentiviral Transduction Particles of nontarget shRNA control and shRNAs for HB-EGF, VEGFA, and ANGPTL4 were purchased from Sigma-Aldrich. The sequences of shRNA used in this study are shown in Supplementary Table S2. Cells were seeded in 48-well plates (50%–60% confluence) and transduced with shRNA-expressing lentiviral particles at an multiplicity of infection (MOI) of 10. After overnight incubation, media was replaced and cells were incubated for a further 24 hours. Stably infected cells were generated by selection with puromycin (1 μg/mL) for 48 hours and used in xenograft models.

Histology and immunofluorescence microscopy

Frozen cryosections of subcutaneous tumors from xenograft models were stained with hematoxylin and eosin (H&E) and stained for immunologic assessment of HB-EGF, VEGFA, or ANGPTL4 expression. For immunofluorescence analysis, cryosections (10 μm) were fixed in methanol for 10 minutes at −20°C, acetone for 1 minute at −20°C and blocked for 10 minutes with blocking solution (Blocking One Histo; Nacalai Tesque). Sections

Published OnlineFirst February 26, 2013; DOI: 10.1158/1541-7786.MCR-12-0428

were then incubated with goat anti-HB-EGF (1:50), rabbit anti-VEGFA (1:1,600), or rabbit anti-ANGPTL4 (1:100) antibodies at 4°C overnight, followed by incubation with FITC-conjugated secondary antibody (1:100) for 1 hour at room temperature. Sections were also incubated with mouse anti-CD31 (1:50) at 4°C overnight, followed by incubation with Alexa Fluor 555–conjugated secondary antibody (1:6,000) for 1 hour at room temperature. Negative controls were stained in parallel with secondary antibody alone. Sections were counterstained with DAPI nuclear stain and mounted with VECTASHIELD Mounting Medium (Vector Laboratories). Section images were photographed using a fluorescence microscope (Leica-DM 2500) and analyzed by Image-Pro Plus 4.5 Software (Media Cybernetics, Inc.).

Tissue samples

Tissue samples were obtained from 15 patients with TNBC following surgery at the Department of Surgery and Sciences, Graduate School of Medical Sciences, Kyushu University (Fukuoka, Japan), between 2003 and 2011. All patients provided signed, informed consent. This study was approved by the Ethics Committee and Institutional Review Board of Kyushu University. Resected tissues were routinely processed as previously described (18).

Capillary tube formation on Matrigel

HUVECs were plated in 6-well plates (10,000 cells/well) precovered with growth factor-reduced Matrigel (Biocoat Cellware; Becton Dickinson) using EGM without FBS and recombinant human HB-EGF, VEGF, or ANGPTL4. After 24-hour incubation, cells were fixed for 10 minutes in 4% (w/v) paraformaldehyde in PBS and photographed. Differentiation of HUVECs into capillary-like tubes was assessed by counting the number of capillary branches under ×100 magnification by 2 independent investigators.

Endothelial monolayer permeability assay

Endothelial cell monolayer permeability was assessed using an In Vitro Vascular Permeability Assay Kit (Millipore-Upstate Biotechnology). HUVECs were plated at 5×10^4 cells per insert in EGM medium and incubated for 48 hours to reach 100% confluency. Following overnight starvation, 500 and 200 μL of EGM medium containing recombinant protein at the indicated concentration was added to the bottom and top chambers, respectively. After incubation for 30 minutes, the medium was removed. A total of 500 μL of EGM medium and 150 μL of EGM medium with FITC-conjugated dextran was then added to the bottom and top chambers, respectively. After 20-minute incubation, 100 μL of medium was collected from the bottom chamber. The fluorescence of each sample was measured at 535 nm (excitation 485 nm) using a fluorescence plate reader. Data were analyzed as relative fluorescent units.

Cell viability assay

Viable cells were determined by Trypan blue exclusion, using a hemocytometer.

Statistical analysis

The statistical significance of differences between values was assessed using the Mann–Whitney *U* test, Bonferroni *t* test, and Spearman rank-order Correlation. Values of *P* less than 0.05 were considered statistically significant.

Results

Gene expression profiles associated with tumor aggressiveness in TNBC

To examine changes in HB-EGF levels associated with tumorigenesis, we used qRT-PCR to assess the expression of EGF family members in MDA-MB-231 and Hs578T TNBC cells in 3DC and xenograft models. Only HB-EGF and EGFR levels were significantly increased in both conditions, compared with 2DC (Fig. 1A and Supplementary Fig. S1A and S1B). These results suggest that among the EGFR ligands, HB-EGF plays an important role in TNBC tumor development. To identify specific pathways and genes associated with TNBC tumorigenesis, we compared gene expression changes in MDA-MB-231 and Hs578T cells in 3DC and in tumor xenografts, compared with 2DC. We identified 7,568 and 4,375 genes commonly upregulated (>2-fold; $P < 0.05$) in 3DC and tumor xenografts in MDA-MB-231 and Hs578T cells, respectively (Supplementary Fig. S1C). Of these, 981 genes were commonly regulated in both MDA-MB-231 and Hs578T cell lines (Fig. 1B). Analysis of these genes identified 3 proangiogenesis factors, VEGFA, ANGPTL4, and PGDFB (Table 1). To validate the microarray results, we analyzed the expression of *VEGFA*, *ANGPTL4*, and *PGDFB* by qRT-PCR. Expression of *VEGFA* and *ANGPTL4* was significantly increased in 3DC and in tumor xenografts in MDA-MB-231 and Hs578T cells, compared with 2DC (Fig. 1C and Supplementary Fig. S1D). However, *PDGFB* expression was not significantly changed in either 3DC or tumor xenografts compared with 2DC in MDA-MB-231 cells (Fig. 1C). In contrast, *PDGFB* levels were significantly elevated in tumor xenografts but not in 3DC cells in Hs578T cells as compared with 2DC (Supplementary Fig. S1E). We next examined the levels of VEGFA, ANGPTL4, PDGFB, and HB-EGF protein secretion into the culture medium. PDGFB forms homodimers or heterodimers with PDGFA (PDGFBB or PDGFAB, respectively). We observed a significant increase in secreted VEGFA, ANGPTL4, and HB-EGF in 3DC of MDA-MB-231 and Hs578T cells compared with 2DC, however, there were no changes in PDGFBB or PDGFAB levels (Fig. 1D and Supplementary Fig. S1F). Expression analysis of other proangiogenic factors or antiangiogenic factors by microarray or qRT-PCR revealed no significant differences in 3DC or the xenograft model compared with 2DC, in either MDA-MB-231 and Hs578T cells (Supplementary Fig. S1D and S1E and Supplementary Tables S3 and S4). Taken together, these findings indicate that the proangiogenic factors, HB-EGF, VEGFA, and ANGPTL4 may play an important role in tumor development in TNBC.

Published OnlineFirst February 26, 2013; DOI: 10.1158/1541-7786.MCR-12-0428

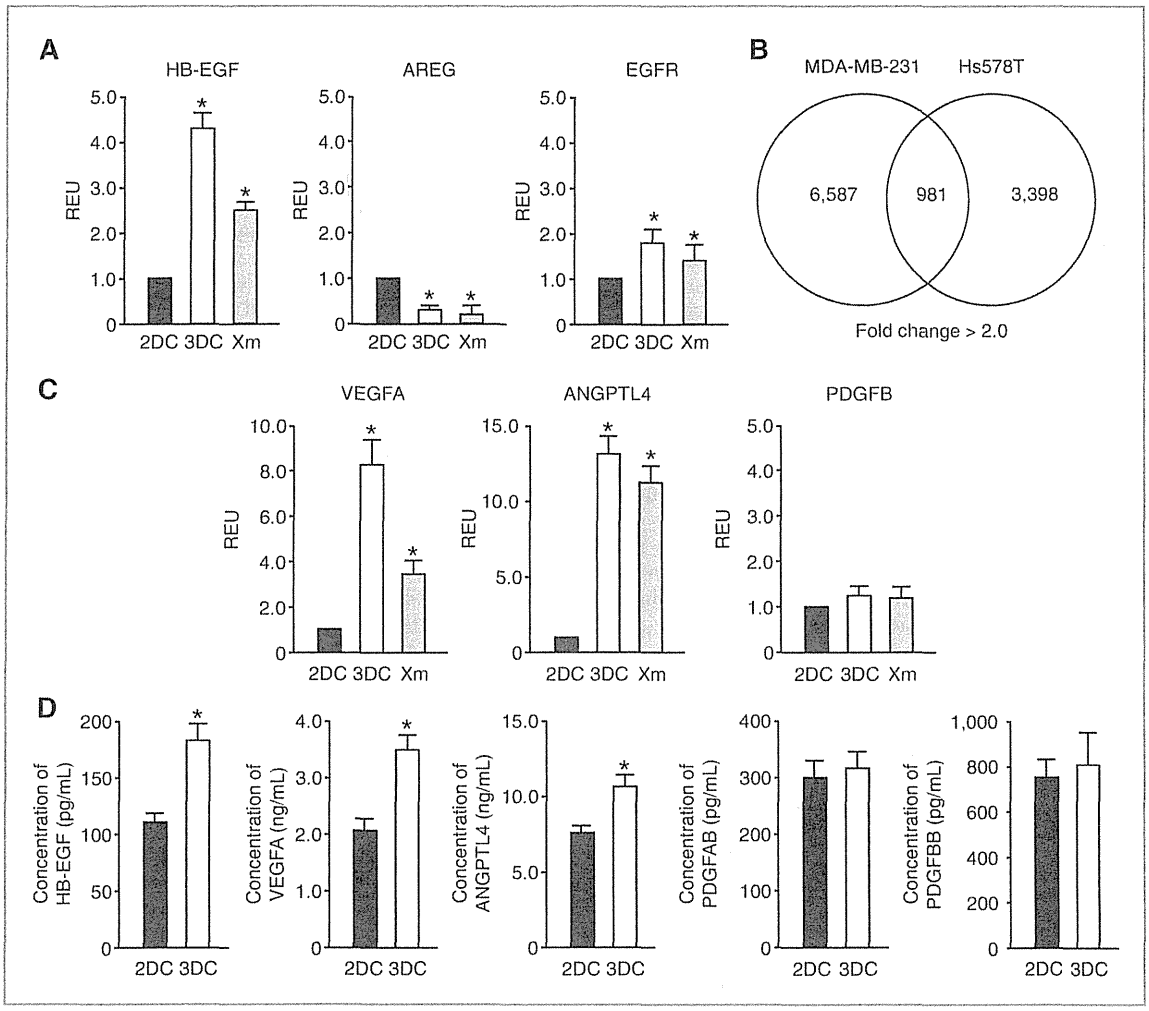

Figure 1. Screening of genes involved in TNBC tumorigenesis. A, expression of EGF family members in MDA-MB-231 cells in 2DC, 3DC, or in tumor xenograft model (Xm). The mRNA expression levels of *HB-EGF*, *AREG*, and *EGFR* were analyzed by RT-PCR. The REU was calculated using 2DC expression as a baseline. B, upregulated genes detected by the expression microarray analysis. Venn diagrams show the number of common genes in 3DC and Xm compared with 2DC in MDA-MB-231 and Hs578T cells (>2-fold). Of these, 981 genes were shared between the 2 TNBC cell lines. The microarray data were found in Gene Expression Omnibus (GEO) database (GEO accession numbers: GSE36953). C, calidation of mRNA expression levels of the angiogenesis-related molecules. mRNA expression levels of *VEGFA*, *ANGPTL4*, and *PDGFB* were analyzed by RT-PCR. The REU was calculated using 2DC expression as a baseline. D, validation of the levels of angiogenesis-related proteins. The expression levels of HB-EGF, VEGFA, ANGPTL4, PDGFAB, or PDGFBB proteins per cell in culture media of MDA-MB-231 under 2DC or 3DC were measured by ELISA and compared with expression levels in 2DC. All values represent the mean and SD of 3 independent experiments (*, $P < 0.05$).

Reciprocal interactions among HB-EGF, VEGFA, and ANGPTL4 through HIF-1α and NF-κB

To investigate the association of HB-EGF, VEGFA, or ANGPTL4 expression with tumorigenesis, we analyzed the effect of targeted knockdown of each of these factors by siRNA in 3DC of MDA-MB-231 and Hs578T cells. Knockdown of HB-EGF led to decreased expression of both VEGFA and ANGPTL4 at both mRNA and protein levels. Conversely, the expression of HB-EGF mRNA and protein was significantly augmented by the inhibition of VEGFA or ANGPTL4 (Fig. 2A and B and Supplementary Fig. S2A–S2F). However, there was no interaction of gene expression between VEGFA and ANGPTL4. To investigate the mechanism by which HB-EGF affects VEGFA or ANGPTL4 expression, we examined the relationship between the expression of HB-EGF, VEGFA, or ANGPTL4 and the activation of HIF-1α or NF-κB. These transcription factors have been previously shown to play a role in the regulation of various proangiogenic factors (26, 27). Silencing of HB-EGF led to a decrease in *HIF-1α* mRNA expression in

Published OnlineFirst February 26, 2013; DOI: 10.1158/1541-7786.MCR-12-0428

Table 1. Upregulated proangiogenic factors in 3DC and xenograft model (Xm) compared with 2DC in MDA-MB-231 and Hs578T cells (>2-fold; $P < 0.05$)

			Fold Change			
	Gene		MDA-MB-231		Hs578T	
Probe set ID	Gene symbol	Gene title	3DC/2DC	Xm/2DC	3DC/2DC	Xm/2DC
211527_x_at	VEGFA	VEGFA	9.53	3.71	2.59	14.68
223333_s_at	ANGPTL4	Angiopoietin-like 4	5.14	5.24	2.52	14.35
204200_s_at	PDGFB	Platelet-derived growth factor β polypeptide	2.96	2.33	2.64	162.52

MDA-MB-231 and Hs578T cells (Fig. 2A and Supplementary Fig. S2A–S2C). We next examined the levels of HIF-1α protein in MDA-MB-231 and Hs578T cells. Nonhydroxy-HIF-1α levels were increased and hydroxy-HIF-1α levels were decreased in 3DC compared with 2DC in both cell lines (Fig. 2C and Supplementary Fig. S2E). Strikingly, inhibition of HB-EGF expression prevented the accumulation of nonhydroxy-HIF-1α protein (Fig. 2C and Supplementary Fig. S2E). Silencing of HB-EGF also led to a decrease in the levels of phosphorylated NF-κB p65 as well as NF-κB inhibitor, although levels of NF-κB p65 mRNA remained unchanged (Fig. 2A and D and Supplementary Fig. S2A–S2C and S2F).

Knockdown of HIF-1α or NF-κB p65 attenuated the expression of VEGFA and ANGPTL4 and led to an increase in HB-EGF expression (Fig. 2A and B and Supplementary Fig. S2A–S2D). Transfection of cells with HIF-1α siRNA significantly diminished expression of nonhydroxy-HIF-1α protein compared with control siRNA, confirming the inactivation of HIF-1α function (Fig. 2C and Supplementary Fig. S2E). Treatment of cells with NF-κB inhibitor significantly suppressed expression of VEGFA and ANGPTL4 proteins, while augmenting levels of HB-EGF (Fig. 2E and Supplementary Fig. S2G). Conversely, knockdown of VEGFA or ANGPTL4 led to an increase in the expression of *HIF-1α* and *NF-κB p65* mRNA and levels of nonhydroxyl HIF-1α and phosphorylated NF-κB p65 proteins (Fig. 2A, C, and D and Supplementary Fig. S2A, S2C, and S2D).

The inhibition of both extracellular signal–regulated kinase (ERK) and AKT attenuated the expression of HB-EGF, VEGFA, and ANGPTL4 (Supplementary Fig. S2H). Suppression of HB-EGF led to a decrease in ERK and AKT phosphorylation (Supplementary Fig. S2I). A significant decrease in the amount of nonhydroxy-HIF-1α or phosphorylated NF-κB was also observed following treatment of *x* cells with AKT inhibitor. The inhibition of ERK also had a suppressive effect on nonhydroxy-HIF-1α accumulation, whereas NF-κB phosphorylation remained unaffected (Supplementary Fig. S2I and S2J). According to these data, the accumulation of nonhydroxy-HIF-1α or NF-κB phosphorylation may therefore be attributed to the activation of ERK and AKT, involved in HB-EGF expression.

In summary, targeted silencing of HB-EGF resulted in a decrease in the active forms of HIF-1α and NF-κB, mediated by ERK and AKT activation, leading to a reduction in VEGFA and ANGPTL4 expression. However, the silencing of HIF-1α or NF-κB induced expression of HB-EGF. Knockdown of VEGFA or ANGPTL4 also induced the expression of HIF-1α, NF-κB p65, and HB-EGF. Taken together, these data indicate that HB-EGF is the central target for suppression of an angiogenic network formed by HB-EGF, VEGFA, and ANGPTL4. The direct inhibition of VEGFA or ANGPTL4 and the indirect inhibition of VEGFA or ANGPTL4 by blocking HIF-1α or NF-κB p65, may induce unidentified transcription factors, leading to enhanced expression of HB-EGF.

Significance of HB-EGF expression in an *in vivo* model of TNBC and in patient samples

To validate HB-EGF as a target for TNBC therapy, we investigated the effect of silencing HB-EGF, VEGFA, or ANGPTL4 on the formation of tumors generated by injection of MDA-MB-231 cells into NOD/SCID mice. Stable knockdown effects of shRNA for HB-EGF (shHB-EGF), VEGFA (shVEGFA), or ANGPTL4 (shANGPTL4) in MDA-MB-231 cells relative to a nontargeting scrambled shRNA (shControl) were confirmed by qRT-PCR (Supplementary Fig. S3A). As expected, the injection of shControl cells into immunodeficient mice led to tumors in all 8 mice (Fig. 3A). However, knockdown of VEGFA or ANGPTL4 led to a significant reduction (~50%) in tumor volume, compared with shControl (Fig. 3A). Even more striking was the effect of HB-EGF knockdown, which inhibited tumor volume by more than 75% compared with shControl (Fig. 3A). We also examined the expression of CD31, HB-EGF, VEGFA, and ANGPTL4 in tumors by immunofluorescence staining. Tumor sections from mice injected with MDA-MB-231 cells infected with either shControl, shHB-EGF, shVEGFA, or shANGPTL4 were assessed at 4 weeks. Expression of CD31, HB-EGF, VEGFA, and ANGPTL4 was markedly diminished in a tumor from shHB-EGF cells, compared with shControl tumors (Fig. 3B and C). Knockdown of VEGFA or ANGPTL4 was associated with weak expression of CD31 in tumors, compared with shControl. In contrast, the expression of HB-EGF in shVEGFA or shANGPTL4 tumors is almost equivalent to shControl

Published OnlineFirst February 26, 2013; DOI: 10.1158/1541-7786.MCR-12-0428

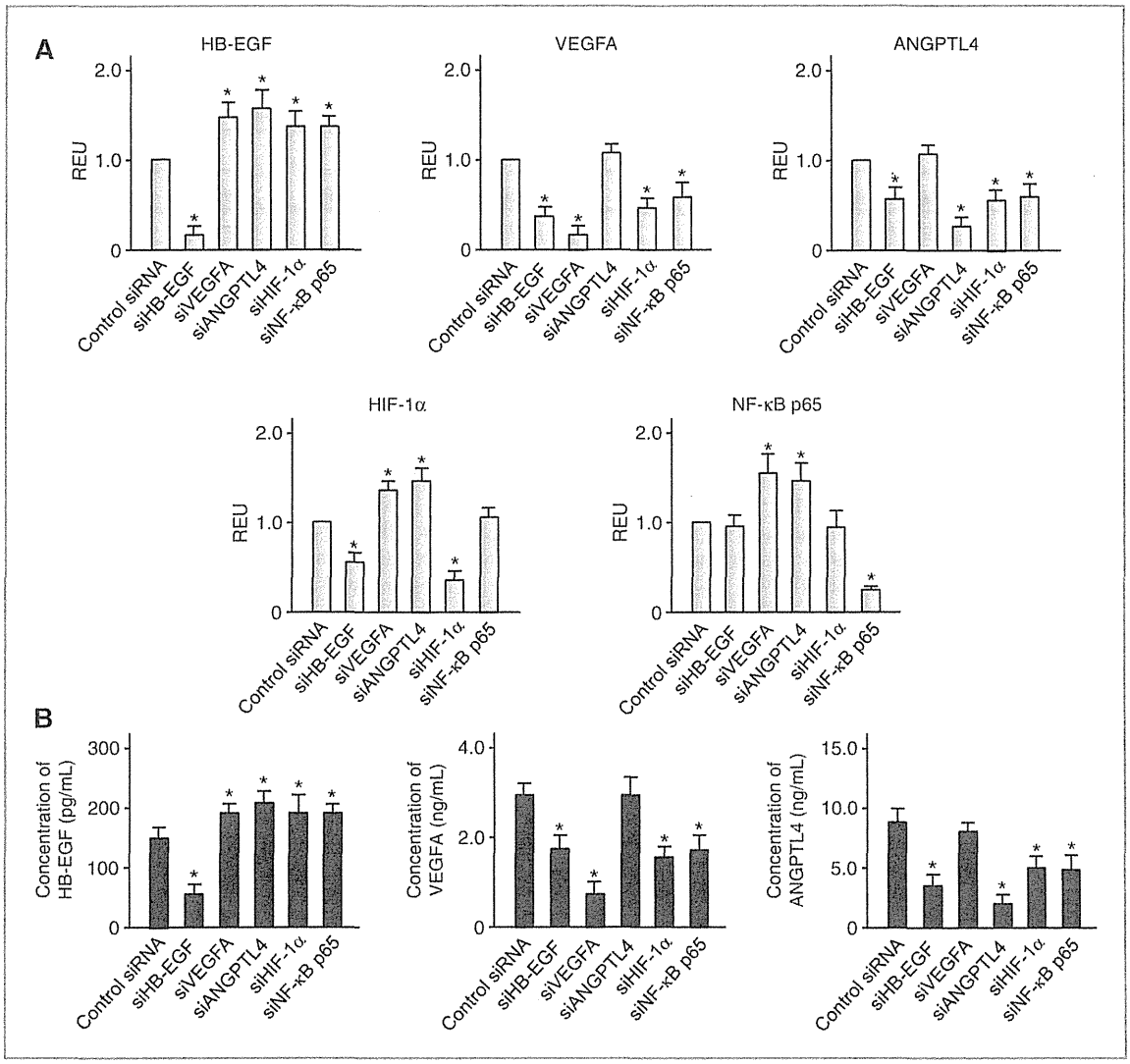

Figure 2. Angiogenesis-related molecules controlled by HB-EGF in 3D proliferation of TNBC cells. Alterations in (A) mRNA expression and (B) protein levels of HB-EGF, VEGFA, or ANGPTL4 under 3DC for 72 hours after transfection with gene-specific siRNAs into MDA-MB-231 cells. The levels of mRNA expression were analyzed by RT-PCR. The REU was calculated using control siRNA expression as a baseline. The levels of HB-EGF, VEGFA, or ANGPTL4 proteins in culture media were measured by ELISA.

tumors (Supplementary Fig. S3B and S3C). Quantitative analysis of HB-EGF, VEGFA, and ANGPTL4 confirmed that expression was also significantly suppressed in xenografted tumors transduced with HB-EGF shRNA, compared with shControl tumors (Supplementary Fig. S3D and S3E). Xenografted tumors derived from cells transduced with shVEGFA or shANGPTL4 exhibited decreased VEGFA or ANGPTL4 expression, compared with control tumors (Supplementary Fig. S3D and S3E). However, the expression of HB-EGF was significantly upregulated in tumor xenografts following knockdown of VEGFA or ANGPTL4 compared with control tumors (Supplementary Fig. S3D and S3E). *PDGFB* expression was not significantly changed in either 3DC or tumor xenografts, compared with 2DC *in vivo* (Supplementary Fig. S3E). Taken together, these *in vivo* data suggest that HB-EGF regulates the expression of VEGFA and ANGPTL4, and that the suppressed function of VEGFA or ANGPTL4 is compensated by HB-EGF upregulation. These results indicate that HB-EGF is associated with tumor formation *in vivo* and may therefore serve as a therapeutic target in TNBC. To validate the clinical significance of HB-EGF in angiogenesis associated with TNBC, we examined the relationship between *HB-EGF* and *VEGFA* or *ANGPTL4* mRNA expression in

Published OnlineFirst February 26, 2013; DOI: 10.1158/1541-7786.MCR-12-0428

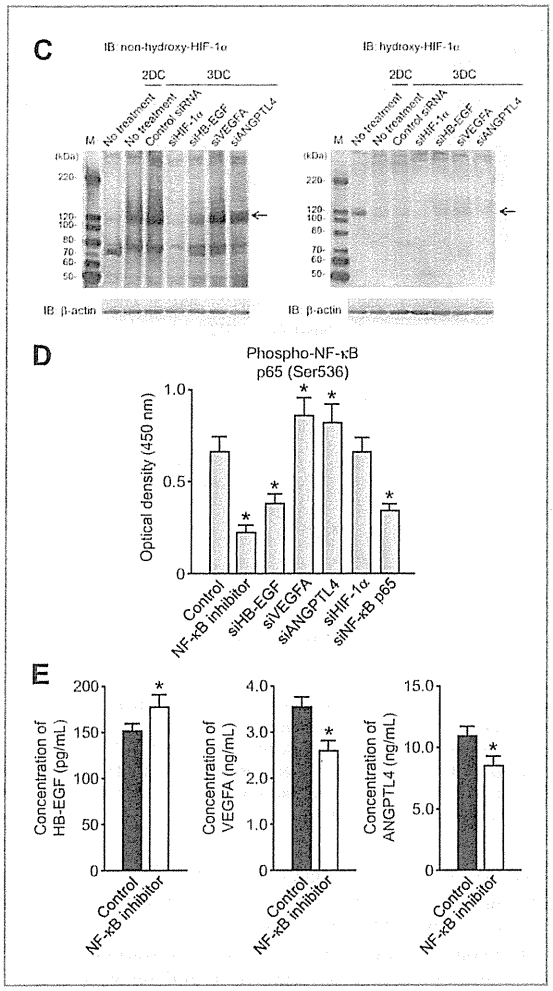

Figure 2. (*Continued*) C, immunoblot (IB) analysis of nonhydroxy-HIF-1α and hydroxy-HIF-1α protein levels in MDA-MB-231 cells under 2DC and 3DC for 72 hours after transfection of gene-specific siRNAs. The bands corresponding to the nonhydroxy-HIF-1α and hydroxy-HIF-1α forms are indicated by the arrows. M, molecular weight marker. β-Actin was used as internal control. Representative data of 3 independent experiments are shown. D, the suppression of NF-κB p65 phosphorylation at Ser536 in MDA-MB-231 cells treated with NF-κB inhibitor versus DMSO control for 72 hours. E, the expression levels of HB-EGF, VEGFA, or ANGPTL4 proteins in culture media after treatment of MDA-MB-231 cells with NF-κB inhibitor or DMSO control for 72 hours by ELISA. All values represent the mean and SD of 3 independent experiments (*, $P < 0.05$).

patients with TNBC. We identified a significant correlation between the expression of *HB-EGF* and *VEGFA* (correlation coefficient = 0.625; $P < 0.01$) or *ANGPTL4* (correlation coefficient = 0.646; $P < 0.01$) in patients with TNBC (Fig. 4A and B). These findings suggest that HB-EGF may modulate both the expression of VEGFA and ANGPTL4 in patients with TNBC. No significant relationships between clinicopathologic characteristics and HB-EGF expression were identified in patients with TNBC (Supplementary Fig. S4 and Supplementary Table S6). However, future studies may require analysis of a larger patient cohort to fully elucidate the relationship between HB-EGF expression and TNBC pathogenesis.

Angiogenic properties mediated by HB-EGF, VEGFA, and ANGPTL4

To evaluate the angiogenic properties mediated by HB-EGF, VEGFA, and ANGPTL4, we examined the effect of these factors on the proliferation and the formation of capillary branches and vascular permeability in HUVECs. HB-EGF (200 pg/mL) and VEGFA (4 ng/mL) similarly induced the proliferation of endothelial cells and the formation of capillary branches (Fig. 5A–C). The effect of ANGPTL4 (15 ng/mL) on the proliferation of endothelial cells and the formation of capillary branches was weaker compared with HB-EGF or VEGFA (Fig. 5A–C). In contrast, ANGPTL4 induced high vascular permeability, compared with HB-EGF or VEGFA (Fig. 5D). The level of angiogenesis induced with 200 pg/mL of HB-EGF, 4 ng/mL of VEGFA, or 15 ng/mL of ANGPTL4 was relatively similar, indicating that signaling through HB-EGF is highly potent. Angiogenesis was not significantly induced using 10-fold lower concentrations of either HB-EGF (20 pg/mL), VEGFA (400 pg/mL), or ANGPTL4 (1.5 ng/mL) alone (Fig. 5E). When used simultaneously at these lower concentrations, however, HB-EGF, VEGFA, and ANGPTL4 promoted vascular permeability (Fig. 5E). These findings indicate that HB-EGF enhances angiogenesis in cooperation with VEGFA and ANGPTL4.

Discussion

In this study, we used gene expression profiling of TNBC cell lines in 3DC and tumor xenograft models to identify 3 proangiogenic factors, HB-EGF, VEGFA, and ANGPTL4, involved in TNBC tumor development. Our analysis shows that HB-EGF lies at the top of a molecular hierarchy of angiogenesis in TNBC, regulating VEGFA and ANGPTL4 through ERK-mediated activation of HIF-1α and AKT-mediated activation of HIF-1α and NF-κB (Fig. 6). We also show that loss of VEGFA or ANGPTL4 seems to stimulate HB-EGF expression, thus functioning as a positive feedback loop. Analysis of *HB-EGF*, *VEGFA*, and *ANGPTL4* mRNA expression coincided with the expression of these proteins by immunofluorescence in xenografted tumors. It is plausible that HB-EGF regulates the expression of VEGFA or ANGPTL4 and that the suppressed function of VEGFA or ANGPTL4 is compensated by upregulation of HB-EGF. ANGPTL4 is recognized as one of several key molecules regulating angiogenesis, functioning as a proangiogenic factor or as an antiangiogenic factor, depending on the cellular context (28–33). In this study, ANGPLT4 expression, which was induced by HB-EGF, was involved in tumor development in our TNBC xenograft model. Moreover, ANGPTL4, in cooperation with HB-EGF and VEGFA, increased vascular permeability in HUVECs. Taken

Published OnlineFirst February 26, 2013; DOI: 10.1158/1541-7786.MCR-12-0428

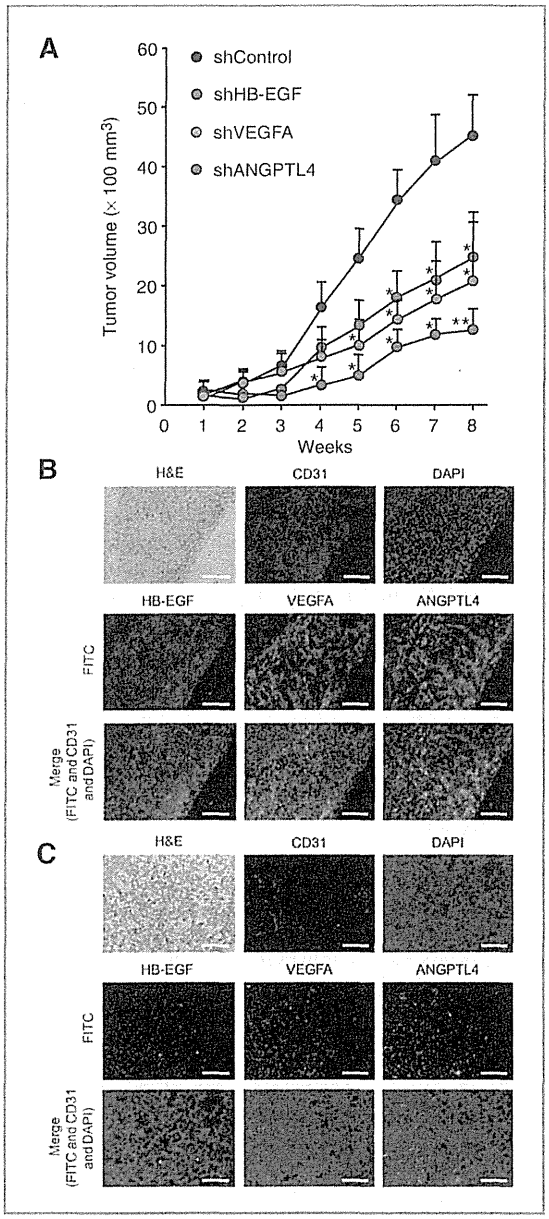

Figure 3. Tumorigenicity of TNBC cells is inhibited by knockdown of HB-EGF and angiogenesis-related molecules. A, tumor growth was measured following injection of mice with MDA-MB-231 cells infected with shRNA against HB-EGF, VEGFA, or ANGPTL4. Data represent the mean + SD of the tumors volumes in 6 mice. *, $P < 0.05$ versus the tumor volume in NOD/SCID mice of control-shRNA group. **, $P < 0.05$ versus the tumor volume in NOD/SCID mice of VEGFA-shRNA or ANGPTL4-shRNA group. H&E and immunofluorescence staining of TNBC xenograft tumor sections from (B) control-shRNA (shControl) and (C) HB-EGF-shRNA (shHB-EGF) mice at 4 weeks. HB-EGF, VEGFA, and ANGPTL4 were stained with FITC (green). CD31, a marker of blood vessel endothelial cells, was stained with Alexa fluor 594 (red). Sections were counterstained with DAPI (blue). Scale bars represent 50 μm.

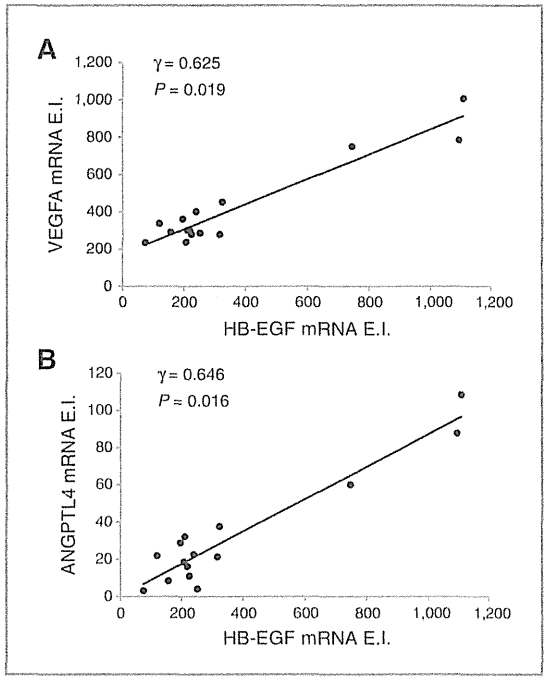

Figure 4. Correlation between expression levels of HB-EGF and angiogenesis-related molecules in patients with TNBC. mRNA expression levels of *HB-EGF* and (A) *VEGFA* or (B) *ANGPTL4* were analyzed by RT-PCR analysis in breast tissue from patients with TNBC ($N = 15$). γ, The Spearman correlation coefficient. $P < 0.05$ were considered statistically significant.

together, these results suggest that ANGPTL4 may play a proangiogenic role in TNBC tumor development in the presence of high HB-EGF expression.

Proteolytic shedding and subsequent activation of angiogenic growth factors, is a process found on various cells during angiogenesis (34). As a consequence, soluble variants are either released into the blood or the vascular tissue. In addition, proteolytic shedding of soluble factors results in an increase in their gene induction. HB-EGF undergoes proteolytic shedding and expression is enhanced by a diverse set of cellular stresses including hypoxia, exposure to UV or chemotherapeutic agents, or inflammatory conditions (35). Transcription factors such as SP1, AP1, c-Fos, and c-Jun have also been associated with induction of HB-EGF expression (36, 37). In this study, the inhibition of VEGFA or ANGPTL4 expression directly or indirectly induced the expression of HB-EGF. Inhibition of VEGFA or ANGPTL4 possibly interrupts the process of neovascularization required for tumor development of TNBC, and the resulting secondary hypoxia may provide cancer cells with DNA damage and mutations essential for cell survival. Such cell stress may evoke the activation of unknown transcriptional factors and the induction of HB-EGF expression as a soluble factor. The enhanced expression of HB-EGF may stimulate the expression of VEGFA and ANGPTL4, resulting in the

Published OnlineFirst February 26, 2013; DOI: 10.1158/1541-7786.MCR-12-0428

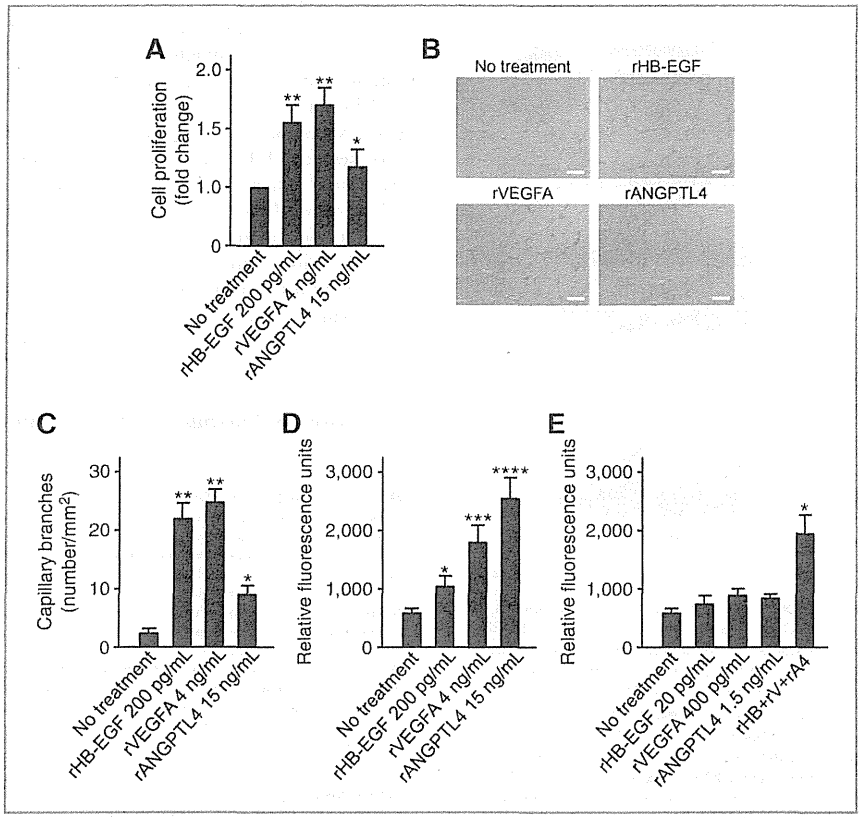

Figure 5. Effect of HB-EGF and angiogenesis-related molecules on vascular endothelial cells. A, proliferation of HUVECs in response to HB-EGF, VEGFA, or ANGPTL4. 2DC of HUVECs were incubated for 24 hours with recombinant human HB-EGF (rHB-EGF; 200 pg/mL), VEGFA (rVEGFA; 4 ng/mL), or ANGPTL4 (rANGPTL4; 15 ng/mL). Viable cells were measured as described in Materials and Methods. Data are expressed as fold change relative to untreated HUVECs. B, representative photographs and (C) quantitative analysis of HUVEC capillary tube formation on Matrigel after incubation with rHB-EGF (200 pg/mL), rVEGFA (4 ng/mL), or rANGPTL4 (15 ng/mL) for 24 hours. Scale bars indicate 100 μm. The numbers of capillary branches were counted in 4 fields of each of 3 wells/condition. D and E, alterations in vascular permeability following stimulation with rHB-EGF (200 pg/mL, 20 pg/mL; rHB), rVEGFA (4 ng/mL, 400 pg/mL; rV), or rANGPTL4 (15 ng/mL, 1.5 ng/mL; rA4) for 30 minutes. Vascular permeability is represented by fluorescence counts. Values represent the mean and SD of 3 independent experiments. *, $P < 0.05$ versus no treatment. **, $P < 0.05$ versus treatment with rANGPTL4. ***, $P < 0.05$ versus treatment with rHB-EGF. ****, $P < 0.05$ versus treatment with rVEGFA.

proliferation of endothelial cells and the disruption of vascular permeability. Thus, molecular hierarchies formed by proangiogenic factors may play an indispensable role in the acquisition of tumor aggressiveness in TNBC.

VEGFA contributes to tumor aggressiveness in a variety of human cancers, and as such, is a rational target for cancer therapy. Contrary to expectations, however, several reports showed that tumor aggressiveness may rebound when VEGFA inhibition ceases, and that VEGF inhibitors also induce tumor hypoxia that may fuel this rebound (38–41). As recently reported in the NSABP C-08 trial, the adjuvant bevacizumab also failed to improve the cure rate of patients with resected colon cancer (42). In addition, there are concerns about the rationale behind using bevacizumab as an adjuvant in other cancer types. Taken together, these studies indicate that the inhibition of VEGFA may not be sufficient to completely suppress tumor angiogenesis in all cancer types. In this study, we show that HB-EGF stimulates the expression of VEGFA and ANGPTL4 as a part of a feedback loop. The expression of these proangiogenic factors may subsequently contribute to tumor formation in TNBC. In ovarian cancer, cross-reacting material 197 (CRM197), a specific inhibitor for HB-EGF, significantly blocked tumor formation and angiogenesis when used in combination with paclitaxel, compared with the combination of bevacizumab with paclitaxel. Accordingly, it will be necessary to develop agents directed against the core or several targets for the successful inhibition of tumor angiogenesis.

To this end, we have developed 2 types of specific inhibitors for HB-EGF, including a biologic material and a neutralizing antibody. In principle, HB-EGF is identified as a diphtheria toxin receptor. CRM197 is a nontoxic mutant of the diphtheria toxin that shares immunologic properties with the native molecule. Thus, CRM197 can bind to the uncleaved form as well as soluble form of human HB-EGF (43). Mechanistically, CRM197 blocks